Defence Research and Development Canada
Recherche et développement pour la défense Canada

DEFENCE R&D DÉFENSE

Computer Aided Dosimetry and Verification of Exposure to Radiation

Edward Waller, Robert Z. Stodilka, Karen E. Leach
and Louise Prud'homme-Lalonde

Defence R&D Canada - Ottawa
TECHNICAL REPORT
DRDC Ottawa TR 2002-055
June 2002

Canada

Computer Aided Dosimetry and Verification of Exposure to Radiation

Edward Waller
SAIC Canada

Robert Z Stodilka
Radiation Effects Group, Space Systems and Technology

Karen E. Leach
Radiation Effects Group, Space Systems and Technology

Louise Prud'homme-Lalonde
Radiation Effects Group, Space Systems and Technology

Defence R & D Canada - Ottawa

Technical Report

DRDC Ottawa TR 2002-055

June 2002

Abstract

In the timeframe following the September 11th attacks on the United States, increased emphasis has been placed on Chemical, Biological, Radiological and Nuclear (CBRN) preparedness. Of prime importance is rapid field assessment of potential radiation exposure to Canadian Forces field personnel.

This work set up a framework for generating an "expert" computer system for aiding and assisting field personnel in determining the extent of radiation insult to military personnel. Data was gathered by review of the available literature, discussions with medical and health physics personnel having hands-on experience dealing with radiation accident victims, and from experience of the principal investigator. Flow charts and generic data fusion algorithms were developed. Relationships between known exposure parameters, patient interview and history, clinical symptoms, clinical work-ups, physical dosimetry, biological dosimetry, and dose reconstruction as critical data indicators were investigated.

The data obtained was examined in terms of information theory. A main goal was to determine how best to generate an adaptive model (i.e. when more data becomes available, how is the prediction improved). Consideration was given to determination of predictive algorithms for health outcome. In addition, the concept of coding an expert medical treatment advisor system was developed.

Résumé

Dans la période suivant les attaques du 11 septembre aux Etats-Unis, une importance accrue a été placée sur la disponibilité opérationnelle au niveau chimique, biologique, radiologique et nucléaire. L'évaluation rapide d'une exposition possible à la radiation sur le terrain est d'une importance capitale pour le personnel des Forces armées canadiennes.

Cette étude a établi un cadre de travail pour la production d'un système informatique "expert" qui aiderait et assisterait le personnel sur le terrain à determiner l'étendue de l'atteinte par rayonnement au personnel militaire. Les données provenaient de la littérature disponible, des discussions avec le personnel médical et le personnel travaillant en radioprotection avec de l'expérience avec des victimes d'exposition au rayonnement, et aussi de l'expérience acquise par le directeur des recherches. Des diagrammes et des algorithmes génériques de fusion de données ont été développés. La relation entre les paramètres connus d'exposition, l'histoire médicale du patient, les symptômes cliniques, les traitements cliniques, la dosimétrie physique, la dosimétrie biologique et la reconstruction de la dose a été évaluée comme indicateurs critiques de données.

Les données obtenues ont été évaluées en terme de théorie d'information. Un des buts était de déterminer le meilleur moyen pour générer un modèle adaptatif (i.e. la possibilité d'ajouter des données, d'améliorer la prédiction). Une considération a été donnée à la détermination d'algorithmes prédictifs sur la santé. De plus, le concept de codage d'un système-conseil en traitement médical a été développé.

Executive summary

In the timeframe following the September 11th attacks on the United States, increased emphasis has been placed on Chemical, Biological, Radiological and Nuclear (CBRN) preparedness. With the knowledge that terrorists are willing to sacrifice themselves for large scale attacks, understanding the consequence and mitigation of radiological attack scenarios are more important than ever. Of prime importance is rapid field assessment of potential radiation exposure to Canadian Forces field personnel.

This work set up a framework for generating an "expert" system for aiding and assisting field personnel in determining the extent of radiation injury to military personnel. The work was not concerned with generating the "expert" system code, but with exploring the data fusion aspects of available information in a semi-quantitative fashion.

The framework was generated by determining the subsets of information required to assist medical personnel in determining extent of radiation injury. Data was gathered by review of the available literature, discussions with medical and health physics having hands-on experience dealing with radiation accident victims, and from experience of the principal investigator. Flow charts and generic data fusion algorithms were proposed. Relationships between the following critical data indicators were investigated:

- Known exposure parameters
- Patient interview and history
- Clinical symptoms
- Clinical work-ups, primarily blood counts
- Physical dosimetry
- Biological dosimetry
- Dose reconstruction

Questions to be answered about the data collected were (a) What is the data used for?, (b) How reliable is the data?, (c) What is the significance of the data collected?, (d) What relationship does a given piece of data have to other data collected?, and (e) What is the temporal significance of the data?

Data was cross-correlated to categorize the quality of the data. Symptomatic and clinical data obtained from prior published radiation accidents was relied upon for estimating risk of exposure. A methodology was explored to incorporate a Monte Carlo radiation transport model for field estimation of whole body and organ biological dose. Both internal and external radiation pathways were considered.

The data obtained was examined in terms of information theory. A main goal was to determine how best to generate an adaptive model (i.e. when more data becomes available, how is the prediction improved). Consideration was given to determination of predictive algorithms for health outcome. In addition, the concept of coding an expert medical treatment advisor system was discussed.

Waller, E., Stodilka, R.Z., Leach, K.E. and Prud'homme-Lalonde, L. 2002. Computer Aided Dosimetry and Verification of Exposure to Radiation . DRDC Ottawa TR 2002-055. Defence R & D Canada - Ottawa.

Sommaire

Dans la période suivant les attaques du 11 septembre aux Etats-Unis, une importance accrue a été placée sur la disponibilité opérationnelle au niveau chimique, biologique, radiologique et nucléaire. Sachant que les terroristes sont prêts à se sacrifier pour des attaques à grande échelle, une connaissance des conséquences et des façons de réduire les impacts des scénarios d'attaque radiologique est plus importante que jamais. Une évaluation rapide de l'exposition potentielle au rayonnement par le personnel des Forces armées canadienne sur le terrain est de la plus grande importance.

Cette étude a établi un cadre de travail pour la production d'un système informatique "expert" qui aiderait et assisterait le personnel sur le terrain à determiner l'étendue de l'atteinte par rayonnement au personnel militaire. Ce travail ne visait pas à développer une système-conseil de codage, mais plutôt à explorer la fusion de données disponibles dans une façon semi-quantitative.

Le cadre de travail a été conçu afin de déterminer les sous-ensembles d'information requis pour aider le personnel médical à déterminer l'étendue de l'atteinte par rayonnement. Les données provenaient de la littérature disponible, des discussions avec le personnel médical et le personnel travaillant en radioprotection avec de l'expérience avec des victimes d'exposition au rayonnement, et aussi de l'expérience acquise par le directeur des recherches. Des diagrammes et des algorithmes génériques de fusion de données ont été proposées. La relation entre les indicateurs de données critiques suivants a été examinée:

- paramètres connus d'exposition
- histoire médicale du patient
- symptômes cliniques
- traitements cliniques, surtout numération globulaire
- dosimétrie physique
- dosimétrie biologique
- reconstruction de la dose

Certaines questions au sujet des données recueillies qui nécessitaient une réponse étaient (a) à quel fin les données seront-elles utilisées?, (b) quelle est la fiabilité des données, (c) quelle est la signification des données?, (d) quelle est la relation entre les différentes données?, et (e) quelle est la signification temporelle des données?

Les données ont été mises en corrélation afin de les classer par catégories. Les données symptomatiques et cliniques obtenues dans des cas d'accidents par irradiation publiés antérieurement ont été utilisées dans l'estimation du risque à l'exposition. Une méthodologie qui utilise le modèle de transport de rayonnement Monte Carlo a été analysée afin de déterminer la dose biologique au corps entier et aux organes.

Les données obtenues ont été évaluées en terme de théorie d'information. Un des buts était de déterminer le meilleur moyen de générer un modèle adaptatif (i.e. la possibilité d'ajouter des données, d'améliorer la prédiction). Une considération a été donnée à la détermination d'algorithmes prédictifs sur la santé. De plus, le concept de codage d'un système-conseil en traitement médical a été développé.

Waller, E., Stodilka, R.Z., Leach, K.E. and Prud'homme-Lalonde, L. 2002. Dosimétrie assistée par ordinateur et vérification d'exposition aux rayonnements. RDDC Ottawa TR 2002-055. R & D pour la défense Canada - Ottawa.

Table of contents

List of figures

List of Tables

1. Introduction

1.1 Background

The Canadian military has been involved in principles of radiation protection and troop dosimetry since the atomic bombs were used in the Pacific theatre war in World War II. As part of this involvement, it has always been a goal to attempt an assessment of the biological radiation dose to troops and the medical treatment paths required after accidental or intentional exposure. Implications to victim triage, LD50, soldier viability to mission completion, medical management and allocation of resources are all fundamental military areas of investigation.

Prior to, and certainly after, the September 11th 2001 terrorist attacks on the United States, other concerns have been brought forward that need to be addressed. Emphasis has shifted from the large-scale nuclear weapon scenario to smaller scale (although potentially lethal) radiation exposure scenarios. Some of these scenarios are outlined in Table 1 (NCRP, 2001).

Table 1 - Current terrorist radiation threats

Radiation Source	Physical size (typical)	Primary Radiation Hazards
Small radioactive source	< mm^3 to > 100 cm^3	External
Large isotopic source	< cm^3 to ~ m^3	External
RDD (large isotopic)	< 500 cm^3 to > m^3	Blast; Internal; External
RDD (spent nuclear fuel)	> m^3	Blast; Internal; External
Commercial power reactor	~ 5 m fuel rod	Internal; External
Research reactor	< 5 m fuel rod	Internal; External
Transportation incident	Various	Internal; External
"Dud" nuclear weapon	Backpacks +	Blast; Internal
Nuclear weapon	Backpacks +	Blast, Thermal; Internal; External

When diagnosing radiation injury severity, it must be noted that radiation exposure manifests itself in certain ways. Table 2 outlines some of the implications to the health care provider in dealing with an ionizing radiation exposure scenario. Although acute radiation insult will not cause immediate death, it is desirable to make increasingly improved estimates of the dose to aid the medical personnel with triage and patient care planning.

The following dose indicator groupings are considered in this report: symptomatology, hematology, physical dosimetry, biological dosimetry and computational dose reconstruction.

Table 2 - Implications of ionizing radiation exposure

Radiation exposure DOES NOT cause	Radiation exposure CAN cause
Immediate death	Nausea, vomiting (~ 1/2 – 48 hours)
Immediate burn wounds	Lymphopenia (~ hours)
A medical emergency	Granulocytosis (~ hours)
A threat to responders	Thrombocytopenia (~ 15 days)
A threat to facilities	Granulocytopenia (~ 15 – 30 days)
Note: *although radiation exposure will not define an emergency, other confounding factors may*.	Immunosuppression (~ 15 days)
	Death from shock (~ 6 hours+)

1.2 Summary of Exposure Pathways for Radiation Injury

There are numerous pathways that external radiation and contamination can interact with the human body. The major pathways of military significance are depicted in Figure 1.

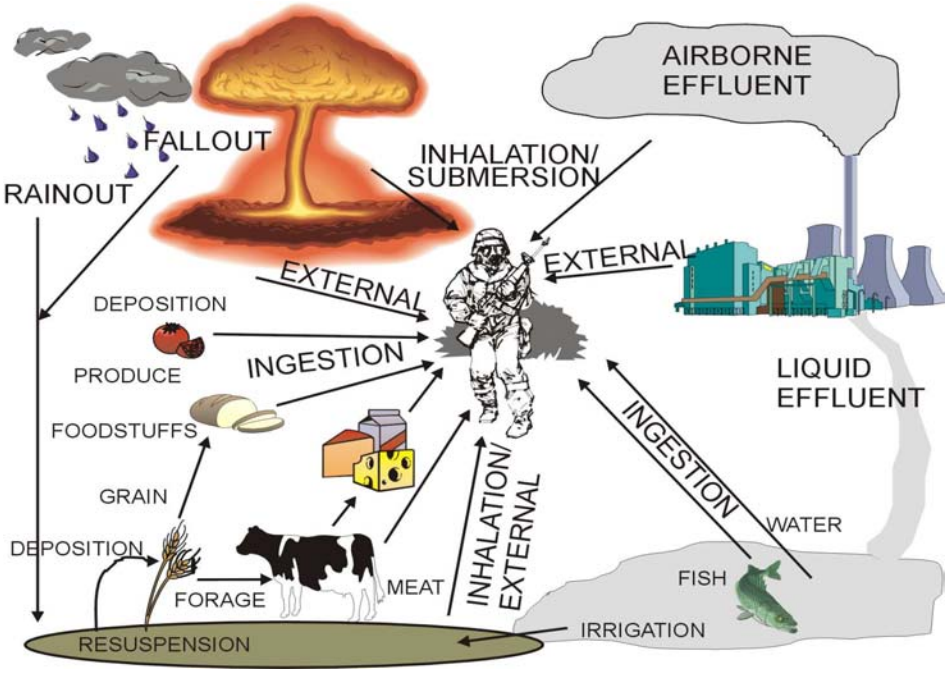

Figure 1 - Exposure pathways

The primary goal for physician-assistant software is the determination of radiation exposure severity to personnel from external radiation fields (typically neutron and gamma), and internal radiation exposure from inhalation and ingestion products (gamma, beta and alpha radiation). It will

be these exposure pathways that are of primary importance when determining acute radiation exposure in the short term, and discussed in this report.

2. Physical Symptomatology

There are two main classifications of radiation insult that may be considered: stochastic and deterministic. Stochastic radiation insult doses do not require immediate medical attention, as the primary long-term effect is increased cancer risk. Therefore, stochastic risk estimation is not considered in the **C**omputer **A**ided **D**ose **A**ssessment and **V**erification of **E**xposure to **R**adiation model - CADAVER. In addition, the symptomatology can be further investigated in terms of:

- Whole-body irradiation; or
- Local irradiation

Whole body and local radiation symptomatology are discussed in the following sections.

2.1 Whole Body Irradiation

Acute radiation exposure can be conveniently divided into two (2) phases: prodromal (initial) phase and manifest (illness) phase. The approximate dose ranges and estimated pathophysiological effects for prodromal and manifest effects are given in Table 3 (adapted from Anno, 1989).

Table 3 - Dose ranges for acute effects

Dose Range (Gy)	Pathophysiological Symptomatology	
	Prodromal	**Manifest**
0.5 – 1.0	Mild	Slight decrease in blood cell count
1.0 – 2.0	Mild to Moderate	Beginning to severe bone marrow damage
2.0 – 3.5	Moderate	Moderate to severe bone marrow damage
3.5 – 5.5	Severe	Severe bone marrow damage
5.5 – 7.5	Severe	Bone marrow pancytopenia and moderate intestinal damage
7.5 – 10.0	Severe	Combined gastrointestinal damage and bone marrow damage; hypotension
10.0 – 20.0	Severe gastrointestinal damage; early transient damage; gastrointestinal death	
20.0 – 30.0	Gastrointestinal and cardiovascular damage	

The expression of severity (mild, moderate, severe) is a qualitative marker, relying upon the reader's medical understanding. For example, mild vomiting or diarrhea can suggest a few episodes, moderate several episodes and severe many profuse episodes. Some effects can be semi-qualitative. For example, mild hypotension may be an approximate 10% drop in blood pressure, whereas severe hypotension can refer to a drop of 30% or more.

Normal symptoms considered within the prodromal phase are:

- Nausea;
- Vomiting;
- Anorexia;
- Diarrhea;
- Fatigue;
- Weakness; and
- Fluid loss/electrolyte imbalance.

Concomitant effects, which may be a result of irradiation or a synergistic result of irradiation and fluid loss, are:

- Headache;
- Fainting; and
- Prostration (exhaustion).

The manifest phase can be characterized by all of the previous symptoms, as well as the following:

- Hypotension;
- Dizziness;
- Disorientation;
- Bleeding;
- Fever;
- Infection;
- Ulceration; and finally
- Death.

The determination of which symptoms have been manifested in a radiation accident victim can be effectuated through a combination of patient interview, observation and diagnostic tests. Although symptomatology is based upon epidemiology, general rules have been developed that may guide the medical care provider in simple determination of acute radiation exposure severity.

Histograms describing some expected symptoms as a function of dose and time of onset are provided in Figure 2 through Figure 8. It is worthy to note here that the observation or absence of any particular symptom(s) does not necessarily preclude irradiation to a given dose range. The data provided allow for broad analysis to be made, which requires supportive data from other more quantitative means before an accurate assessment of dose to patient may be made. Although the symptomatological data is coarse, it is also usually the first data to be collected post-irradiation, and is therefore useful to bound the extent of an exposure incident, and may be extremely useful in the triage of patients in a mass irradiation event.

In the dose range 1-2 Gy, prodromal effects and injury to the hemopoietic system (primarily the bone marrow stem and precursor cells) increase significantly. However, victims will probably survive. There is, however, a 2-5% expected lethality after doses of about 2 Gy. The probability of death increases if victims are already weakened by other conditions, such as pre-existing infection. Although survival is possible within 2-3.5 Gy, prodromal effects become pronounced. Victims also suffer moderate to severe bone marrow damage. As the dose reaches approximately 3.5 Gy, 50% who did not receive appropriate medical care may die within 60 d. From 3.5-5.5 Gy, symptoms are more severe, affecting nearly all exposed. If untreated, it is expected that 50-99% may die, primarily because of extensive injury to the hemopoietic system, manifested by overwhelming infections and bleeding. Responses to doses between 5.5 and 7.5 Gy begin to reflect the combined effects of gastrointestinal and hemopoietic damage. Survival is almost impossible short of a compatible bone marrow transplant and/or extensive medical care. Nearly everyone irradiated at this level suffers severe prodromal effects during the first day after exposure. Between 7.5 and 10 Gy, injuries are much more severe due to greater depletion of bone marrow stem cells, increased gastrointestinal damage and systemic complications from bacterial endotoxins entering the blood stream. At 10 to 20 Gy, early transient incapacitation may become more frequent. Death results in less than 2 wk from septicemia due to severe gastrointestinal injury, complicated by complete bone marrow damage and the cessation of granulocyte production. Above approximately 13 Gy, death may occur sooner from electrolyte imbalance and dehydration due to vomiting and diarrhea., especially in hot or humid conditions. Extremely severe gastrointestinal and cardiovascular damage causes death within 2-5 d after doses of 20-30 Gy.

Post-exposure mortality is estimated by the incidence of fatalities and the period over which they are likely to occur for a given dose level. The dose-mortality relationships are discussed as follows:

- **0.5 - 1 Gy** Acute radiation effects at this level are mild and occur only during the first day after exposure. Blood cell counts may drop slightly, but typical victims will surely survive.

- **1 - 2 Gy** Between 20 and 70% of exposed persons develop nausea and vomiting; as the dose approaches 2 Gy, 50% or more of exposed persons developed anorexia, nausea and vomiting. About 30-60% complain of fatigue and weakness. Significant destruction of bone marrow stem cells may lead to a 20-35% drop in blood cell production. As a result, mild bleeding, fever and infection may occur during the fourth and fifth post-exposure weeks. Up to 5% may die 5-6 weeks post-exposure to 2 Gy.

- **2 - 3.5 Gy** Commencing in this dose range, approximately 10% may experience one or two episodes of moderate diarrhea 4-6

hour post-exposure. Most victims tire easily and experience mild to moderate weakness intermittently over the 6 weeks. Under normal conditions, vomiting and diarrhea are not enough to cause serious fluid loss and electrolyte imbalance. In hot or humid conditions, however, fluid loss without replacement and electrolyte imbalance could become serious. Injury to the hemopoietic system is indicated by moderate bleeding, fever, infection and ulceration 3-5 wk post-exposure; more than 50% of those exposed are affected. During the fourth and fifth weeks, moderate diarrhea may complicate their condition. Five to 50% of non-treated persons may die during the fifth week; death comes earlier to those with pre-existing infections, such as infections of the upper respiratory tract.

- **3.5 - 5.5 Gy** The onset and duration of nausea, vomiting and anorexia are about the same as in the preceding dose range, but the symptoms are more severe and affect nearly all exposed persons. Severe and prolonged vomiting can take a toll on electrolyte balance, which may be accelerated by perspiration through heat, humidity or activity. About 10% may experience moderate to severe diarrhea 3-6 hours post-exposure. Nearly all show moderate to severe fatigue and weakness for many weeks. If untreated, 50-99% may die, primarily because of extensive injury to the hemopoietic system, manifested in overwhelming infections and bleeding during 3-6 weeks. Nausea, vomiting and anorexia may recur at that time. Diarrhea, electrolyte imbalance and headaches affect at least half. The condition of the lethally irradiated during their terminal days may be complicated by dizziness, disorientation, fainting, prostration and symptoms of infection and bleeding.

- **5.5 - 7.5 Gy** Virtually all exposed persons experience severe nausea and vomiting the first post-exposure day, moderating over the next day or two. During that time, they also experience dizziness and disorientation. With the near maximum destruction of bone marrow stem cells and absence of granulocytes, untreated persons lose their defense against infection. By the end of the first post-exposure week, infection is rampant from endogenous bacteria that have escaped from the injured gastrointestinal tract. The combination of hemopoietic damage and gastrointestinal lesions reduces the survival of all untreated persons to 2-3 weeks. During the entire time, they suffer from severe fatigue and weakness. Toward the end of the first week, nausea, vomiting and anorexia recur. Moderate to severe diarrhea may begin as early as 4 days. Severe bleeding, headaches, hypotension, dehydration, electrolyte imbalance and fainting complicate the conditions of all prior to death.

- **7.5 - 10 Gy** The survival time for untreated persons diminishes to 2 - 2.5 weeks. Symptoms resemble those experienced at the preceding dose range, with the following notable differences:
  - Severe nausea and vomiting may continue into the third day before moderating;
  - During the first day, hypotension affects about 80%; moderate fever for 30-45%;
  - Electrolyte imbalance is a persistent problem from 6 hours on;
  - All have moderate to severe headaches during the first day; and
  - Nearly three-quarters are prostrate before the end of the first week.
- **10 - 20 Gy** Severe nausea and vomiting affect all within 30 min of exposure and continue intermittently, along with anorexia, until death the second week. Severe headaches begin after about 4 hours and continue for 2-3 days. Symptom severity may diminish somewhat during days 3-5. Gastrointestinal injury predominates, manifested 4-6 days post-exposure by the abrupt return of severe nausea, vomiting, anorexia and diarrhea, along with high fever, abdominal distension and undetectable peristalsis. During the second week, severe dehydration, hemoconcentration and circulatory collapse, compounded by septicemia, lead to coma and death.
- **20 - 30 Gy** Symptoms are more severe versions of those described for the preceding dose range. Gastrointestinal injury predominates, complicated by cardiovascular lesions. Prodromal effects, including severe headache and drowsiness, appear almost immediately after exposure and may persist as the gastrointestinal syndrome develops. Severe dehydration and electrolyte imbalance are manifested several hours after exposure, but in time the greater loss is from severe diarrhea. The increased permeability of capillaries in the intestines and elsewhere in the body releases fluids into the interstitial spaces.

The data presented in Figure 2 through Figure 8 may be converted to simple algorithms and used in a data fusion computer code.

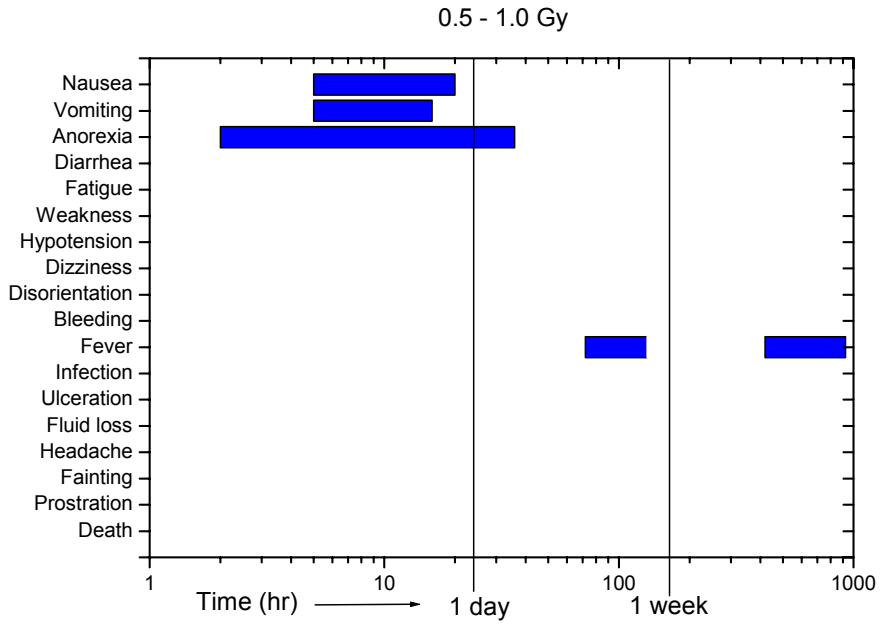

Figure 2 - Symptoms for 0.5 - 1.0 Gy

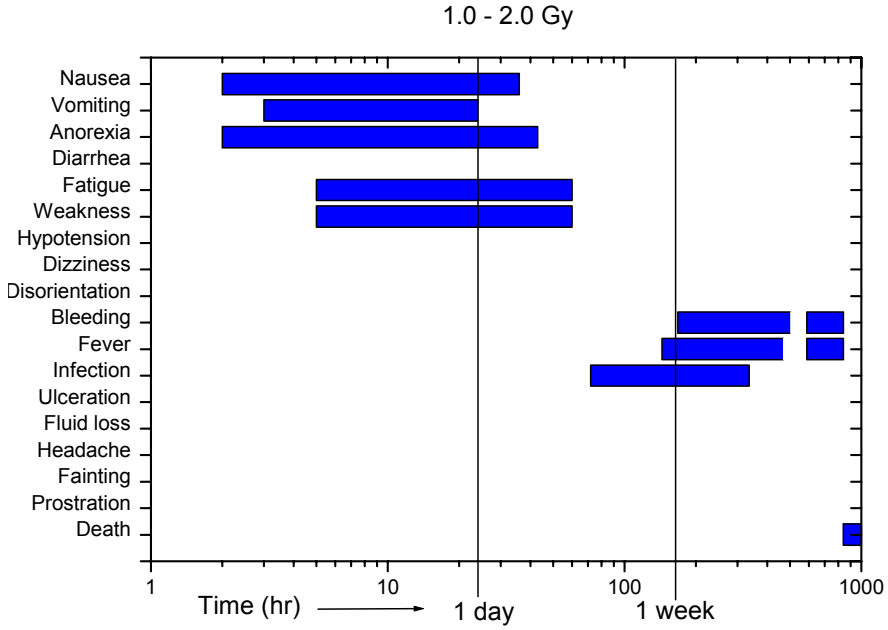

Figure 3 - Symptoms for 1.0 - 2.0 Gy

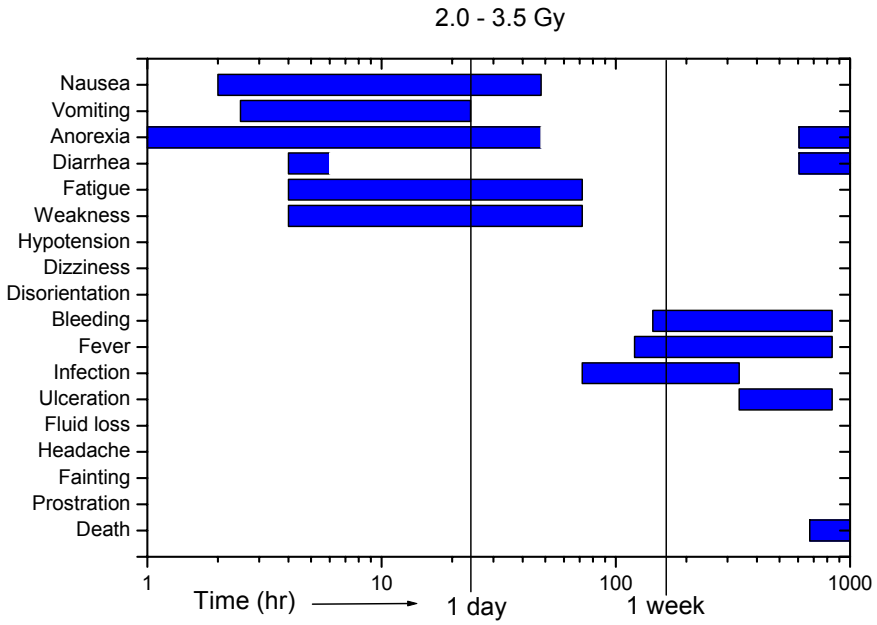

Figure 4 - Symptoms for 2.0 - 3.5 Gy

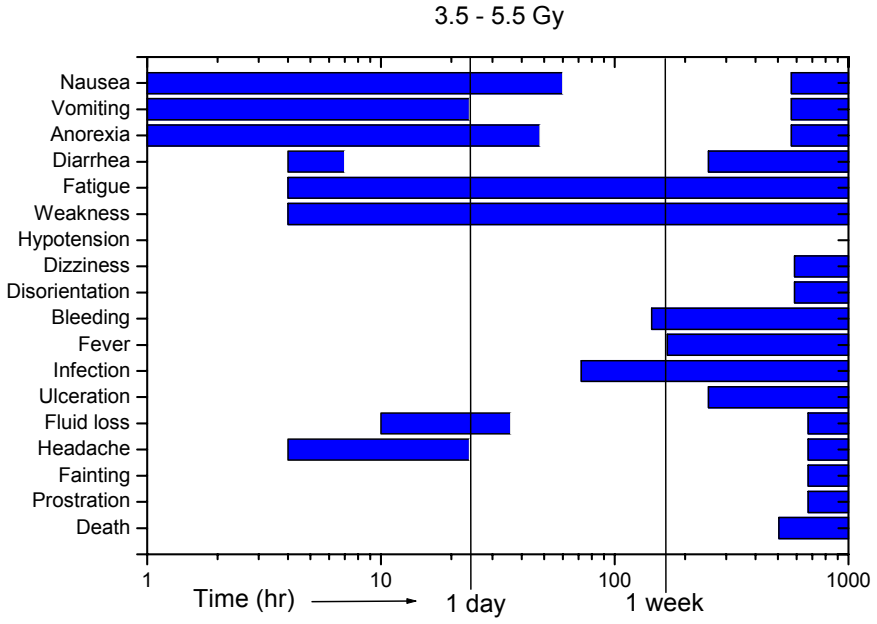

Figure 5 - Symptoms for 3.5 - 5.5 Gy

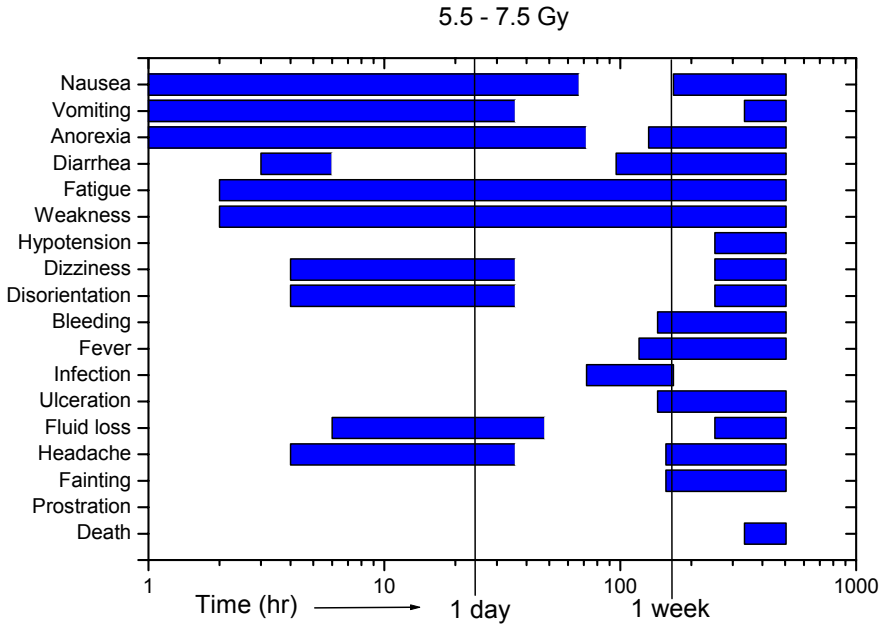

Figure 6 - Symptoms for 5.5 - 7.5 Gy

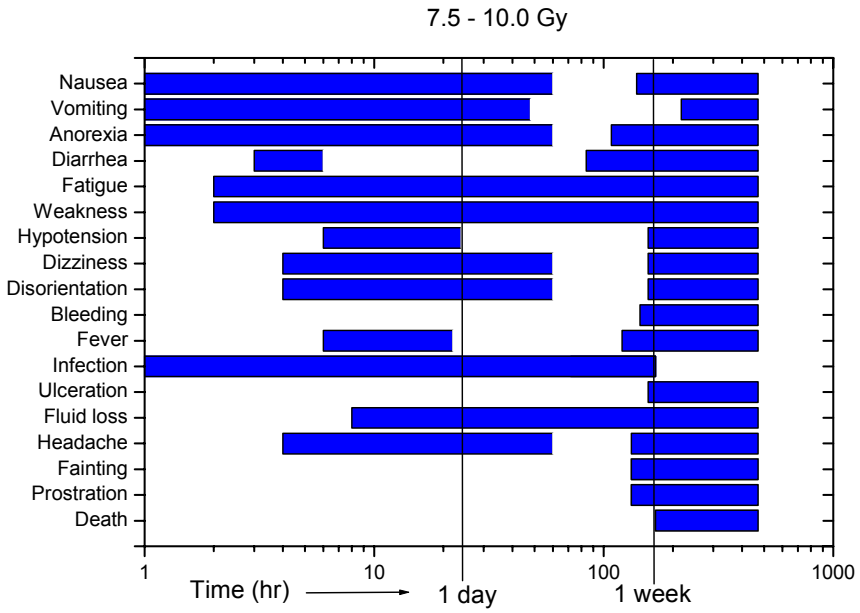

Figure 7 - Symptoms for 7.5 - 10 Gy

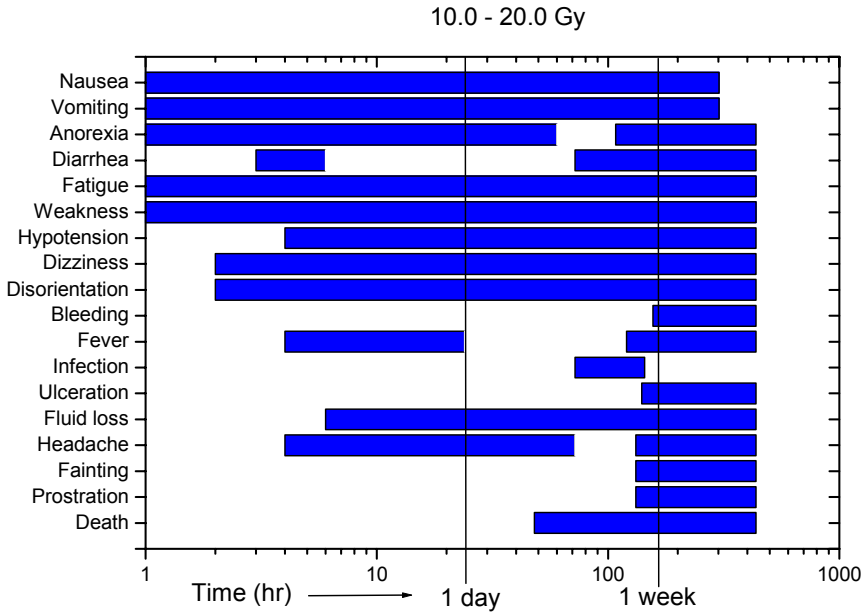

Figure 8 - Symptoms for 10.0 - 20.0 Gy

2.2 Local Irradiation

Physical dosimetry is important for determining the severity of partial body or local irradiation, since no appropriate biodosimetric method is available for the early stages of local radiation injury. A detailed history of the accident should be taken and recorded. As regards physical examination, skin reaction should be observed daily with the aid of serial colour photo documentation.

The use of electron spin resonance methods can be helpful to estimate the dose incurred when applied to teeth, clothes, buttons, earrings, or any organic substance exposed. During the first week following an accident, daily blood counts can help to discount the possibility of whole body exposure, since in local radiation injury only certain non-specific changes can be observed such as mild leukocytosis. Chromosomal aberration may be found in only a small number of cultured lymphocytes at a local exposure with a dose range of 5-10 Gy (IAEA, 1998). The different methods, in terms of practicality and postulated cost, are discussed in detail in Section **4.4**.

There are two primary diagnostic procedures used to assess the severity of local over-exposures: thermal and radioisotopic methods. Both are most reliable when the irradiated area can be compared with a corresponding unirradiated one, and are qualitative in nature. The approximate time of onset

of symptoms characteristic of local injury, dependant upon the dose received, is outlined in Table 4.

Table 4 - Symptomatology for local radiation injury

Symptom	Dose range (Gy)	Time of onset (days)
Erythema	3-10	14-21
Epilation	> 3	14-18
Dry desquamation	8-12	25-30
Moist desquamation	15-20	20-28
Blister formation	15-25	15-25
Ulceration	> 20	14-21
Necrosis	> 25	>21

Although the range of various symptoms for local radiation insult are described in Table 4, the scale of severity of the symptoms are generally the same as for common thermal burns: erythema, oedema, blisters, ulceration, necrosis and sclerosis (IAEA, 1988), described in the following.

Erythema

Reddening of the skin
Can arrive early, transistory or late (6-18 months)

Oedema

The topography of the early oedema gives indication of the volume irradiated, but does not enable its boundaries to be demarcated precisely. Usually oedema is hot, hard, red, taut, shiny and accompanied by paraesthesia. The initial oedema appears between the first and the 21st day; and the higher the dose the earlier its appearance. However, no clear correlation can be established between the dose and the date of appearance. The late oedema (several weeks, months or years after exposure) precedes and accompanies increases in vascularization. Its duration varies.

Blisters

These are characteristic lesions affecting the basal layer of the epidermis. Topographical and dimensional analysis of blisters is of interest for dosimetry. The periphery of the blister corresponds to a skin dose of between 15 and 25 Gy. The chronology of blister development depends on the dose received by the basal layer - the higher the dose, the shorter the time before the blisters appear: a lag time of 21 days corresponds to a surface dose of 12 to 20 Gy. The blisters subside and heal, evolving then, as a function of the dose absorbed in depth, either towards cutaneous restoration or towards necrosis.

Necrosis

This occurs at doses above 25 Gy. It begins with ulceration, the ulcers formed being fairly deep with a yellowish base covered with a fibrinous exudate. Their appearance may change, becoming blackish when dried out (dry gangrene). The onset of necrosis occurs from several weeks to several months.

Sclerosis

Sclerosis occurs in muscular, tendon and aponeurotic tissues. The higher the dose, the earlier it sets in. As it is retractile, it presents functional problems, chiefly in the fingers and palms of the hands. It may lead to deformity, the hands becoming fixed in a *claw-like* position with the fingers hooked. In addition, annular sclerosis can develop on the phalanges causing oedema distal to the constriction.

3. Hematopoietic Considerations

3.1 Blood Pathophysiology

In simplified terms, the blood is formed from two components: liquid and formed. The liquid component is termed the plasma, and the formed components are the erythrocytes, leukocytes and thrombocytes which are suspended in the plasma. To better understand radiation insult to the hematopoietic system, the differential components of blood are discussed in this section.

Plasma The plasma carries antibodies and nutrients to the tissues, and carries waste products away;

Erythrocytes Also called red blood cells (RBC), carry oxygen to the tissues and remove carbon dioxide from them;

Leukocytes Also called white blood cells (WBC), participate in the inflammatory and immune system response; and

Thrombocytes Also called platelets, work in unison with the coagulation factors in plasma to control clotting.

3.1.1 Plasma

Plasma is a translucent, straw colored fluid that consists primarily of the proteins albumin, globulin and fibrinogen. The components of plasma regulate acid-base balance, immune response of the body, assist nutrition and accelerate blood coagulation. Important products that circulate in plasma include urea, uric acid, creatinine and lactic acid. As such, plasma may be investigated for total creatinine content, which has been studied recently in depleted uranium incorporation scenarios. However, the plasma does not provide much useful information for acute radiation exposure in the early stages.

3.1.2 Erythrocytes

In adults, red blood cells are usually formed in the bone marrow. Red blood cell production is regulated by the tissue's demand for oxygen and the blood cells' ability to deliver it. Erythrocyte formation begins in a precursor called a stem cell, which eventually forms into a red blood cell.

3.1.3 Leukocytes

White blood cells protect the body against harmful bacteria and infection. They are generally classified as either:

- Granular leukocytes (or, granulocytes), such as neutrophils, basophils and eosinophils; or
- Non-granular leukocytes, such as lymphocytes, monocytes and plasma cells.

Although most white blood cells are produced in the bone marrow, lymphocytes and plasma cells complete maturity in the lymph nodes.

Neutrophils are the predominant form of granulocyte, making up approximately 60% of the total white blood cell inventory. They surround invading organisms and foreign matter. The other granulocytes defend against parasites, participate in allergic reactions (by releasing heparin and histamine into the blood) and fight lung/skin infections. Since radiation appears as an "insult" to the blood, the neutrophils spike initially to combat this. The rapid break-down in other systems depletes the neutrophil population, and is based on severity of insult. This blood component is, therefore, an important marker of radiation injury severity.

Monocytes, along with neutrophils, devour invading organisms. They also migrate to tissues where they develop into cells called macrophages that participate in cell immunity.

Lymphocytes form into two type: B cells and T cells. The B cells produce antibodies and the T cells regulate cell-mediated immunity. The lymphocytes, and specifically the T-cells, get depleted rapidly after radiation insult, and therefore are excellent markers for radiation injury severity in the early stages.

Plasma cells, which develop from lymphocytes in tissues, produce, store and release antibodies.

3.1.4 Thrombocytes

Platelets are small, colorless disk shaped cytoplasmic cells that are split from cells in the bone marrow. They have a short life span (~ 10 days) and they perform three vital functions: shrinking damages blood vessels to minimize blood loss, forming plugs in injured blood vessels, and accelerate blood coagulation. When tissue injury occurs, blood vessels at the injury site constrict and platelets clump to prevent hemorrhage. Since thrombocytes do not decrease as rapidly as other blood indicators, they are not as desirable for a primary marker of radiation injury severity.

3.2 Radiation Response of Hematopoietic System

The degree of injury is generally proportional to radiation dose. There is typically very little variability in the response of different persons to a given dose and only a moderate degree of biological variation, except for rare instances of hypersensitivity associated with preexisting disease.

A set of total-body radiation syndromes has been described for humans, relating symptoms, laboratory changes, and outcome to the severity of injury. There has been very little human experience with the effects of high radiation doses, except in Japan and to a certain extent the former Soviet Union, where the data are incomplete and complicated by combined injury effects. Some of the human syndrome descriptions are based on inadequate data, or are partially extrapolated from results in experimental animals. It is possible, however, to make medical plans on the basis of this incomplete information.

Subclinical injury requires little description. A known history of exposure can be based on radiation monitors and demonstrated levels of exposure in the environment. Sensitive laboratory changes consist of small numbers of chromosome changes, which are expensive to demonstrate because of the large number of cells that must be analyzed. A delayed fall in sperm count may also show quite low doses. Less sensitive and less specific is the slight decrease in absolute lymphocyte count. In all of these tests sequential values from serial tests are likely to improve sensitivity, and in all, the possible effects of factors other than radiation cause difficulties in interpretation.

The *hematopoietic syndrome* is represented by fairly plentiful data in humans. It consists of alterations in hematopoiesis due to damage of stem cells in marrow and lymphatic tissue. The changes may vary from mild to lethal. A decrease in lymphocytes occurs promptly, most of it taking place within 24 hr after exposure (see Figure 9). The level of this early lymphopenia is one of the best indicators of severity of radiation injury. The level of neutrophil granulocytes shows a very early rise, usually limited to the first 48 hr or less; the degree of its elevation has not been correlated with the extent of injury, as depicted in Figure 10 (In the neurovascular syndrome, granulocytosis is very pronounced and persists until death). In the dose range that produces the hematopoietic syndrome, after the early rise, granulocyte numbers fall to fairly low levels at about day 10, and there is then a transient, abortive rise at around day 15, perhaps due to mitoses of a genetically damaged population that cannot continue to reproduce. The absence of an abortive rise is an unfavorable sign for the patient. Thereafter, a steady fall in granulocyte count begins, with the nadir at about day 30 post-exposure. If the patient survives, this is followed by spontaneous recovery, beginning in the fifth week. The platelets may show a rise in the first 2 or 3 days after exposure, then a gradually accelerating decrease with the nadir also reached at about day 30. During recovery the platelets are likely to bounce up well above normal levels (Andrews, 1980).

The *gastrointestinal syndrome* is not well documented in humans. It has been believed to result mainly from radiation inhibition of mitosis of the cells in the crypts of the intestine, with electrolyte loss from the mucosa, and extensive bacterial invasion there. Clinically, it is characterized by severe, persistent nausea, vomiting, and diarrhea, in addition to manifestations of a very profound hematopoietic syndrome. Death is estimated to occur during the second week after exposure. However, studies of total-body radiation given clinically to facilitate marrow grafts (at dose rates below those likely to occur in accidents) suggest that in man quite high doses can be given without producing this syndrome.

The *neurovascular syndrome* occurs when extremely large doses of total-body irradiation are received, and it has been seen in two persons accidentally irradiated. It is characterized by pronounced neurological disturbances, after an early interval of mental alertness. Intractable hypotension is a prominent feature and may be the major basis for the neurological changes rather than direct radiation damage to the brain as was earlier proposed. There is early onset of severe nausea, vomiting, and bloody diarrhea. Lymphocytes fall promptly to near-zero levels, and pronounced leukocytosis develops early and persists until death at perhaps 2 to 5 days after exposure.

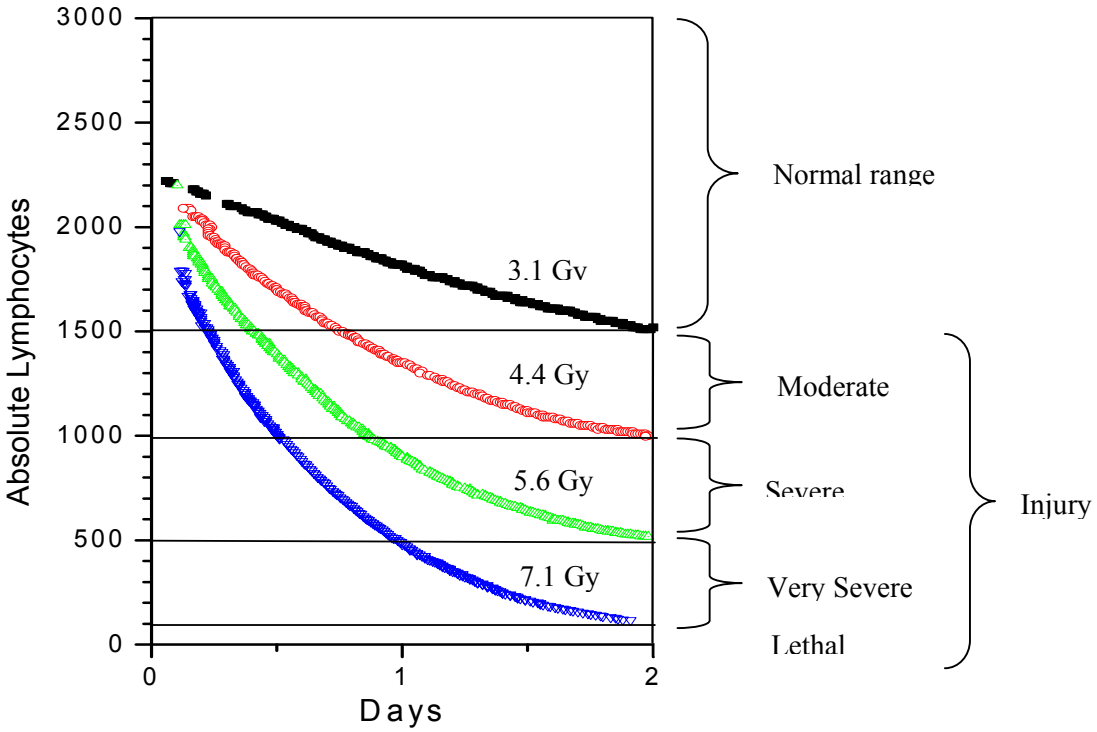

Figure 9 - Patterns of early lymphocyte depletion for radiation insults

There are several interesting aspects to the series of blood changes depicted in Figure 10. One is the pronounced delay in reaching the nadir in granulocytes and platelets. This cannot be accounted for entirely on the basis of the time

periods involved in normal blood cell kinetics; much more rapid patterns are seen with some marrow-damaging cancer chemotherapeutic agents. The radiation changes do appear to be at least indirectly related to normal intervals of cell dynamics, however, and occur much more rapidly in small experimental animals than in man. The time sequence is not altered in relation to radiation dose as much as might be expected. With exposure levels causing a severe hematopoietic syndrome, the onset of pronounced granulocyte and platelet depression is earlier, but the time of recovery is only slightly delayed.

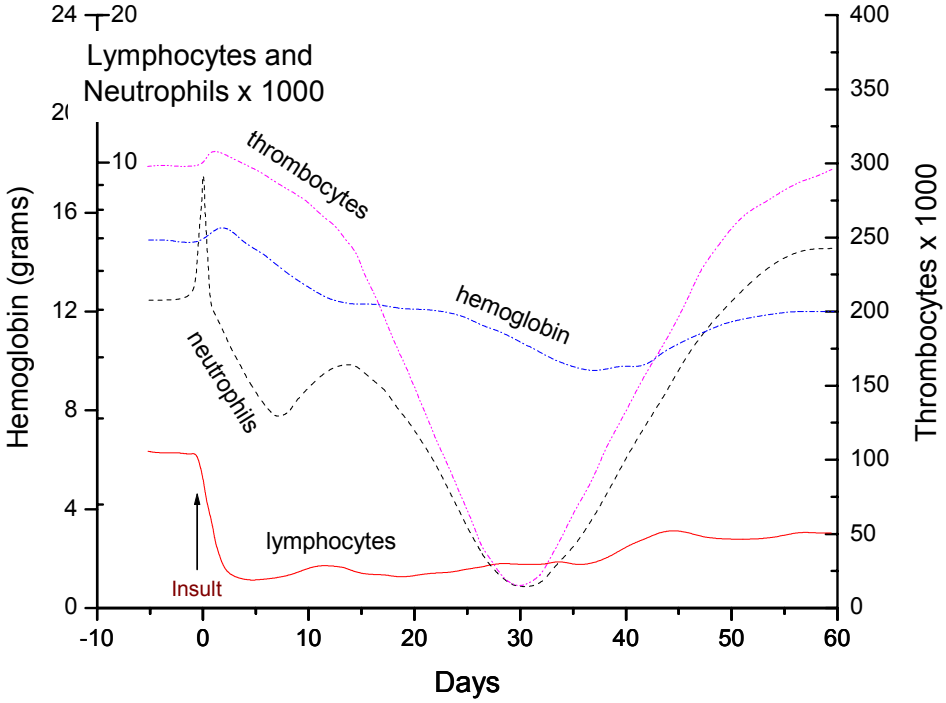

Figure 10 - Typical acute radiation syndrome complete blood count with differential

It may be seen that although many of the manifestations of acute whole body irradiation are semi-qualitative, the absolute differential blood counts may be used to estimate degree of severity of exposure.

3.3 Modeling Blood Dynamic

Biological estimates of radiation injury are of great value in radiation accidents, and should outweigh the physical dosimetry in guiding therapy. A number of studies have been performed which deal with modeling blood dynamics post-irradiation. Referring to Figure 10, it may be seen that there are two primary hematopoietic indicators that may be measured early after

acute radiation insult: change in lymphocytes and change in neutrophils (specifically, granulocytes). Although thrombocytes (or, platelets) are significant with respect to blood clotting, the severe change in the ability of the body to combat infection (granulocytes) and produce new healthy blood cells (lymphocytes) are better primary indicators of severity of radiation insult.

As indicators of degree of injury, blood studies are preferable to marrow studies. Even if patients would tolerate bone marrow aspirations once or twice a day, the information would not be as useful as frequent blood counts. The marrow is less amenable to quantitative measurements, and even when the irradiation dose is uniform, the marrow shows variability from site to site as it does in the normal person. When the radiation exposure is non-homogeneous, it is of course impossible to judge the overall hematopoietic status from a marrow specimen. During the first few days after an accident, the marrow may look and test normal, and this may cause an underestimate of the degree of injury.

The following sections discuss both qualitative and quantitative aspects of blood dynamics modeling.

3.3.1 Qualitative Blood Dynamic

Lymphocytes The absolute lymphocyte count will fall within a few hours after significant radiation exposure, with most of the decrease occurring during the first 48 hours. At 48 hours an absolute lymphocyte count of greater than 2000/mm^3 generally suggests that there has been no life-threatening dose. Between approximately 1200/mm^3 and 2000/mm^3 suggests a significant, yet probably non-lethal dose. Less than 1200/mm^3, a serious dose. Below 500/mm^3 a possibly lethal dose, and below 100/mm^3 almost certainly a lethal dose. After the initial decrease in numbers, the lymphocyte levels tend to remain relatively stationary, and in non-lethal doses there is a slight increase toward normal after about 30 days (Andrews, 1973).

Neutrophils The neutrophil count may rise transiently within a few hours, and very high values suggest severe injury. It is believed that stress-induced release of cells already formed must account for the spike. The more commonly described manifestation, leukopenia, begins to be prominent after a few days. At sub-lethal dose levels, there may be a plateau, or even a slight temporary rise, in neutrophil values at around ten days to two weeks. The most severe leukopenia develops during the third and fourth weeks, to be followed by a fairly rapid return to normal. At higher radiation doses the plateau or temporary rise may not be seen and the leukocyte count may be very low by the second week; when this happens the prognosis is extremely poor. During the fifth or sixth week, spontaneous recovery is expected to begin.

Thrombocytes Changes in thrombocyte values tend to be very similar to those in the neutrophils. After maximum depression has been passed, the regenerative output of thrombocytes (usually starting in the fifth or sixth week) may be more striking than that of the granulocytes and may include a temporary rise to above normal values.

Erythrocytes Early changes in the red cell values of the blood may be caused indirectly by dehydration. An anemia due to marrow damage takes some weeks to develop and reaches its greatest severity just as leukocyte and platelet values are beginning to recover. The anemia is usually mild unless there is significant bleeding; however, a decrease in iron utilization immediately after exposure indicates a distinct decrease in red cell formation, even with rather small doses of total body irradiation. During the recovery phase from high dose, there is a definite reticulocyte response, reaching its peak between 45 and 50 days after exposure.

Interpreting blood count values to estimate degree of injury in managing an accident would require the care-provider to have available the published records of blood values in other accidents, or a physician diagnosis tool. During the first 48 hours the lymphocyte fall would be of greatest value. Although there is indication that early granulocyte rise can be used to quantify the degree of injury in the sub-lethal dose range, it is not suitable as a unique marker because of different responses in different victims. A very high granulocyte count which continues to rise after 24 hours suggests a lethal exposure. In less severely injured patients, after the first 4 or 5 days it may be assumed that the greater the fall in granulocytes the more serious is the injury, and failure to show a plateau or rising value around days 10 to 16 is typically a fatal sign. Once the severe marrow depression sets in at two to three weeks post-exposure, the care-provider can observe the degree of granulocyte and platelet depression, observing until day 30 after which spontaneous recovery can be expected.

3.3.2 Quantitative Blood Dynamics

Both lymphocytopoiesis and granulocytopoiesis have received special interest in recent years because of the fact that they are the most important quantitative indicators for acute radiation exposure in the first days after an accident (see Section 3.3.1). Biomathematical models can be used as a nucleus for a medical decision support system for the treatment of irradiated persons. Work performed by numerous investigators (see, for example Hofer & Tibken (1994), Tibken & Hofer (1995), and Hofer et al (1995)) have shown that linked ordinary differential equations may be used to describe the dynamics of both lymphocytes and granulocytes in the blood. The models are complex, and lend themselves to matrix solution.

In most simple terms, the blood can be modeled as a single compartment, depicted in Figure 11.

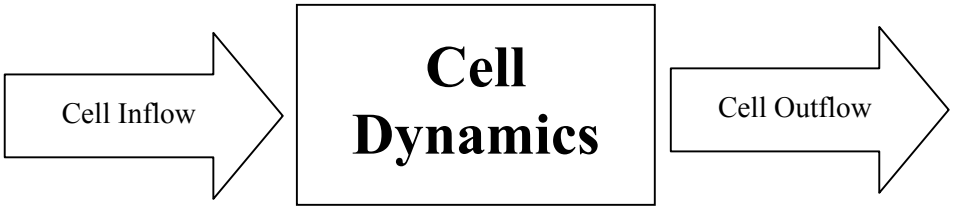

Figure 11 - Single blood compartment

The resulting differential equation governing the cell dynamics for this system is given as

$$\frac{dx}{dt} = u(t) - y(t) + \alpha \cdot x(t)$$
$$y(t) = \lambda \cdot x(t)$$

where x(t) represents the total number of cells at time t, u(t) represents the cell inflow and y(t) represents the cell outflow. The cell outflow rate is represented by λ and the cell production rate by α, which must be estimated through observation or experimental data to solve the equation.

Models become increasingly complex as more blood compartments are incorporated. For example, the anatomical compartments required to model lymphocytopoiesis are seen in Figure 12. Within each compartment, lymphocyte compartments are further sub-defined based upon B-cell and T-cell characteristics.

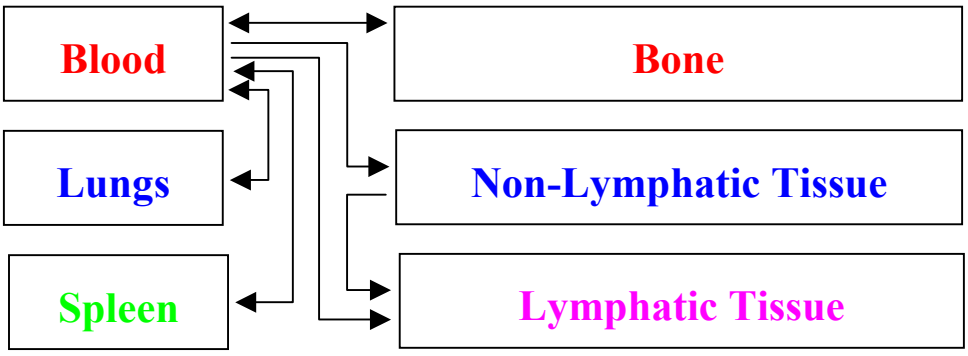

Figure 12 - Lymphocytopoiesis compartment model

For granulocytopoiesis, an even more complex compartment model is required, as depicted in Figure 13.

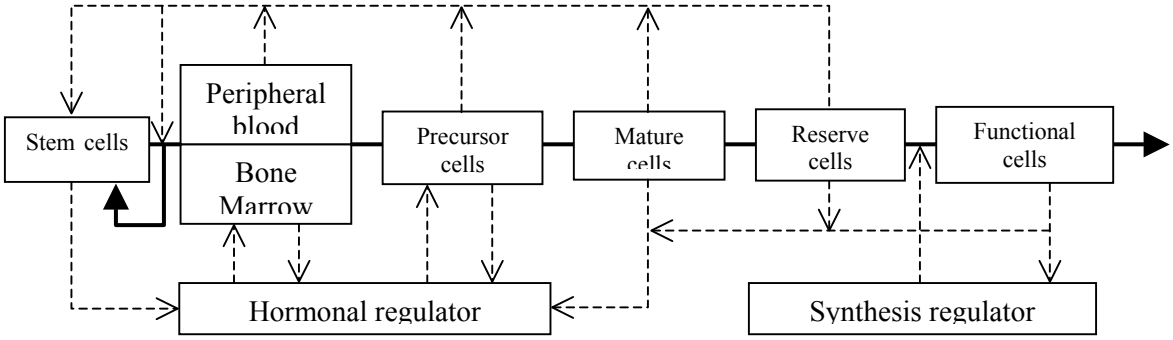

Figure 13 - Granulocytopoiesis compartment model

As an example, Tibken and Hofer (1995) used a multi-compartmental blood model and multiple differential equations to estimate granulocyte kinetics from radiation accidents in Chernobyl and Israel. The results they obtained are presented in Figure 14.

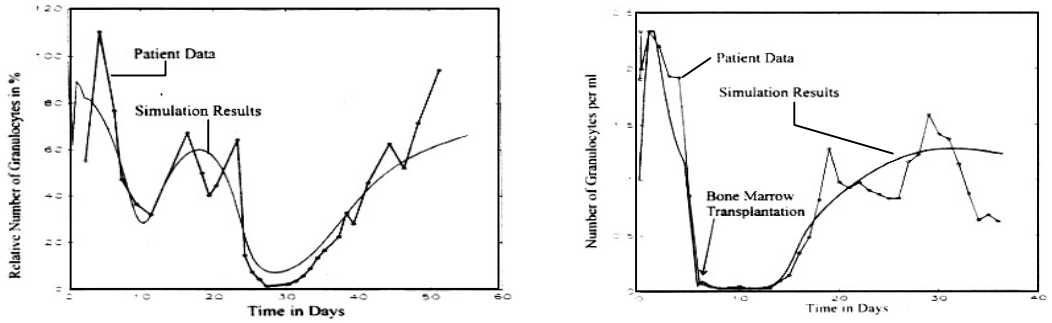

Figure 14 - Granulocyte dynamics modeling for acute irradiation exposure in Chernobyl (L) and Israel (R)

Although the above formulation can be used for stem cell research, it has limited applicability for field diagnosis of acute radiation insult[1].

Work by Goans et al (1997) has focused on modeling early (< 8 hour) lymphocyte depletion following acute radiation insult. The lymphocytes have been shown to disappear from the peripheral blood after acute radiation exposure as follows:

[1] Although this is true in the current form of the biomathematical models studied, this does not preclude the possibility of reducing/simplifying the differential equations to provide adequate estimates of lymphocyte and granulocyte dynamics, without requiring a large number of state parameters to be assigned.

$$L(t) = L_0 e^{-K(D)\cdot t}$$

where L_0 is the lymphocyte count pre-accident (1500 ~ 4500/mm^3), L(t) is the lymphocyte count post-exposure at time t, and K(D) is a rate constant.

If it is possible to estimate the rate constant by obtaining serial blood counts taken in the first few hours post exposure, then it is possible to estimate the acute radiation dose (i.e. plotting $L(t)/L_0$ on a natural logarithm scale versus time, and obtaining the slope of the curve (-K))

Goans et al (1997) obtained curves of lymphocyte depletion as a function of time, at a given dose, and determined a rate constant for each. The rate constants were plotted as a function of dose, reproduced in Figure 15. This data was fit by Goans using a weighted Levenberg-Marquardt non-linear regression to obtain a dose response relationship as

$$D = \frac{a}{1 + \left(\frac{b}{K}\right)}$$

where a = 13.6 and b=1.0, with a coefficient of determination (r^2) of 0.83. The fit is valid for K ~ 0 to 7 days^{-1}. A more simple third order polynomial was fit to this data by the author, valid for K ~ 0 to 3 day^{-1}, and is given as

$$Dose(Gy) = A + B \cdot K + C \cdot K^2 + D \cdot K^3$$

where A = 0.27869, B = 10.34289, C = -4.29884 and D = 0.65614. The coefficient of determination (r^2) for this fit is 0.998.

This simple model may be effectively used to predict dose, if complete blood counts (CBC) are taken repeatedly within approximately the first ½ day post-exposure. After this time, the model is not valid. It may be possible to use simplified biomathematical models to achieve the same goal, and perhaps extend the timeframe of validity.

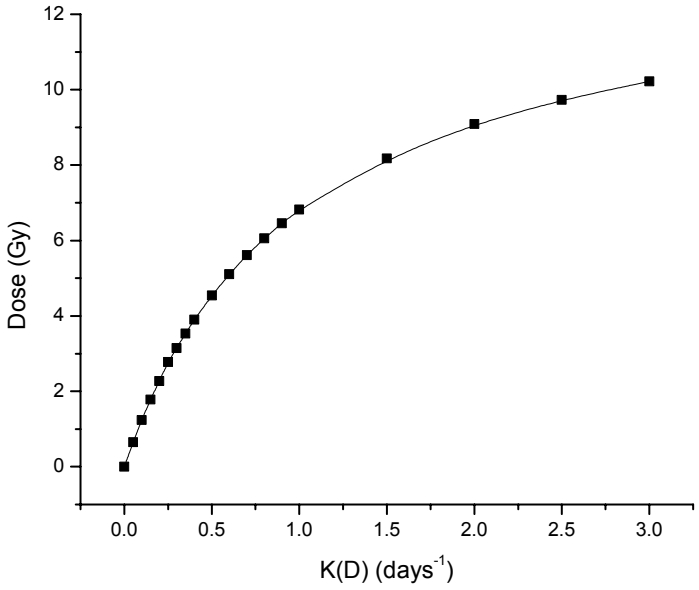

Figure 15 - Lymphocyte depletion rate constant as a function of dose

The most simple lymphocyte expressions may be derived from first-order exponential fits to the estimated lymphocyte depletion described in Figure 9. The equation governing this is:

$$\left|L(t)\right| = A + Be^{-t/C}$$

where |L(t)| is the absolute lymphocyte count at time t (days), and A, B and C are first order constants related to dose, defined in Table 5. By following lymphocyte depletion in a radiation accident patient, and matching exponential coefficients, a range of exposure may be identified.

Table 5 - First order exponential constants for lymphocyte depletion

Constant	Dose (Gy)			
	3.1	**4.4**	**5.6**	**7.1**
A	800.36	765.21	310.47	-28.70
B	1470.56	1511.43	1913.83	2117.34
C	2.69	1.04	0.86	0.70

4. Dosimetry

There are three (3) major classifications of dosimeters that may provide useful information for physician-assistant software:

- physical dosimeters;
- biological dosimeters, and
- opportunistic dosimeters

The three classifications are discussed in the following sections.

4.1 Physical Dosimetry

Physical dosimetry herein is discussed in terms of materials and techniques that allow determination of an estimated biological dose.

4.1.1 TLD

Thermoluminescent Dosimeters (TLD) are the most commonly used physical dosimeters. TLDs are generally issued to personnel performing radiation work and are classified as Nuclear Energy Workers (NEW) by the Canadian Nuclear Safety Commission (CNSC). TLDs can be configured to measure neutron and gamma radiation dose (and in some cases, beta radiation). The sensitivity of the TLD depends upon the type of TLD used and the orientation of the TLD with respect to the source of radiation. The TLD dose is generally assigned as a whole body dose, unless the dosimeter is used in a specific fashion, such as a ring dosimeter, which would have its dose recorded as an extremity dose. If a TLD is available after a radiation exposure, this provides an important basic dose measurement, to which other dose estimates will be compared. The TLD is considered a passive, integrating dose-measuring device.

4.1.2 EPD

An electronic personal dosimeter (EPD) provides much of the same function as a TLD, although it is capable of providing more information. The EPD is generally only used to determine a gamma dose. Depending on the type of EPD, other information may be available such as dose and doserate time logging. This information may be important to determine potential fractionation of dose, which affects the severity of the dose and the medical treatment path. The EPD, like the TLD, has sensitivity dependant upon the orientation with respect to the source of radiation. The EPD is considered to be an active, integrating and spot dose/doserate-measuring device.

4.1.3 Survey

The primary purpose of radiation survey meter readings in assessing radiation exposure severity is when performing an *a posteriori* survey of a radiation source, fallout field, etc. The radiation survey meter will allow the health physicist to determine gamma and/or neutron doserates, and also α/β contamination levels (using appropriate probes). This method of dose estimation is more appropriately termed dose reconstruction, and is most useful for external radiation fields and relatively long-lived radioactive isotopes. In addition to radiation survey meters, other types of dose estimation may be appropriate, such as air sample counting, or spectroscopic or liquid scintillation analysis of samples (such as swipes, clothing samples, etc). Blood counting for ^{24}Na after neutron irradiation is considered in Section 4.1.6.

4.1.4 Whole Body Counting

A whole body counter can be used to estimate radionuclide activity incorporated by a victim of an inhalation or ingestion scenario. Determination of incorporated activity is required to estimate the committed dose equivalent, which can be used in physician-assistant software. Whole body counters are not typically available in the field, due to their size and weight, and therefore whole body data will normally become available at times greater than approximately 24 hours post-exposure.

4.1.5 ESR

Electron Spin (or Paramagnetic) Resonance can be defined as either a physical or biological dosimeter, depending upon where the sample is obtained. EPR dosimetry is applicable over many orders of magnitude in absorbed dose ($10^{-2} \sim 10^{5}$Gy) and using biological tissues (bone; tooth enamel) or inanimate materials (clothing; pottery), retrospective dose assessment and mapping can be accomplished. EPR for radiation dosimetry is a highly specialized application of this technique, and therefore an EPR estimate of absorbed dose will be a unique input to physician-assistant software.

4.1.6 Special Case – Neutron Irradiation

The radiation dose that an accident victim receives from neutrons can be estimated by measuring the radioactivity induced in the victim, the victim's clothing, or in articles the victim might be wearing or carrying.

Several techniques can be useful for identifying personnel exposed to neutron radiation. In most facilities where significant quantities of fissionable materials are present, the required personnel dosimetry badge worn by an

employee has a detector element (generally an indium strip) specifically designed for neutron measurements. When the indium strip is activated, the radiation emitted from it can be measured with a GM survey meter. It is possible to establish a rough "calibration" curve relating the neutron dose to a survey meter reading at contact with the indium strip. But most use the meter reading only as an indicator of significant exposure to neutrons, since total dose so strongly depends on factors such as neutron spectrum, gamma/neutron ratio, and orientation of personnel. One technique of dose estimation is by surveying for the neutron-induced activation of metallic items such as coins, watches, rings etc. to triage (or, "quick-sort") people into exposed or non-exposed groups, which will assist in prioritizing other measurement techniques such as both bioassay and whole body counting.

Table 6 lists some common elements and their activation products for fast neutrons. Because of the short half-lives of many metals, metals should be checked as soon as possible after exposure, and Table 7 lists common elements and their activation products for thermal neutrons.

Table 6 - Threshold reactions for fast fission neutrons

Reaction	Isotopic (%)	Threshold E_n (MeV)	σ (b)	Half-life	Emission Type	Radiation min^{-1} g^{-1} per Gy fission neutrons
$^{31}P(n,p)^{31}Si$	100	2.7	0.03	2.6 h	$\underline{\beta}$	7.15E+04
$^{31}S(n,p)^{32}P$	95	2.8	0.065	14.2 d	β	1.09E+03
$^{24}Mg(n,p)^{24}Na$	79	7.2	0.0013	15.0 h	$\underline{\gamma}$	5.44E+02
$^{27}Al(n,\alpha)^{24}Na$	100	7.3	0.0006	15.0 h	γ	2.84E+02
$^{27}Al(n,p)^{27}Mg$	100	4.7	0.032	9.5 m	γ	1.44E+06
$^{58}Ni(n,p)^{58}Co$	67	2.8	0.111	71.0 d	γ	1.37E+02
$^{115}In(n,n)^{115m}In$	96	1.2	0.174	4.5 h	γ	3.09E+04

Table 7 - Threshold reactions for thermal neutrons

Reaction	Isotopic (%)	σ (b)	Half-life	Emission Type	Radiation $min^{-1} g^{-1}$ per Gy fission neutrons
$^{55}Mn(n,\gamma)^{54}Mn$	100	13.2	2.6 h	γ	5.00E+02
$^{63}Cu(n,\gamma)^{64}Cu$	69	4.5	12.8 h	β	1.04E+04
$^{68}Zn(n,\gamma)^{69}Zn$	19	0.097	13.8 h	γ	1.03E+04
$^{68}Zn(n,\gamma)^{69}Zn$	19	1	57 m	β	1.05E+04
$^{109}Ag(n,\gamma)^{109m}Ag$	49	3.2	253 d	γ	1.02E+04
$^{107}Ag(n,\gamma)^{108}Ag$	51	45	2.3 m	β	1.08E+04
$^{197}Au(n,\gamma)^{198}Au$	100	98.8	2.7 d	γ	5.00E+02
$^{115}In(n,\gamma)^{116m}In$	96	150	54.0 min	γ	1.08E+04

Other samples, such as the hair, which contains approximately 5% sulfur may assist in dose estimation since some of the stable sulfur will be activated by fast neutrons to radioactive ^{32}P. Samples of urine, fingernails, and toenails, as well as certain items of clothing, may also be analyzed for radioactivity.

A crude method for estimating a neutron dose is to use a GM survey meter as a "whole body counter" by placing the survey meter at the person's waist, and having the person bend over (another "quick sort" method). The following relationships apply very roughly for relating the meter's response to neutron dose:

a) $1\,\text{cGy} \cong 100\,\text{cpm}$

This applies when measured *immediately after* exposure to fast neutrons. This is modified to 1 cGy ~ 50 cpm at approximately 15h after exposure to fast neutrons following decay of ^{38}Cl.

b) $\text{Dose(cGy)} \cong 800{,}000 \cdot \chi_R\,(mSv/hr)/Wt(lbs)$

This gives an estimate of whole body dose.

c) $\text{Dose (cGy)} \cong 3 \cdot \text{CR(cpm)}/Wt(lbs)$

This gives an estimate of whole body dose.

When using the GM survey meter method, remember that external contamination can be confused with ^{24}Na ($t_{1/2}$ = 15 h) activity and result in considerable overestimation of dose. Also, a reading taken immediately after an acute exposure will be higher by a factor of about 2 due to the ^{38}Cl ($t_{1/2}$ =

37 min) activity that will be present. This can cause confusion and an over-estimation of the dose if not accounted for when using this method. A better estimate of the neutron dose can be made with a properly calibrated whole body counter.

For physician assistant software, this type of parametric estimate can be incorporated. It is worthy to note that for every neutron exposure, there is also a corresponding gamma component requiring estimation.

4.2 Biological Dosimetry

Biological dosimetry is important because physical dosimeters may be:

- Erroneously exposed while not being worn;
- Obstructed during exposure;
- Absent during exposure; and
- Lost or damaged during processing.

Some biological dosimeters include:

- Lymphocyte depression;
- Nausea/vomiting;
- Epilation;
- Erythema; and
- Induction of chromosome aberrations

Of the biological dosimeters described above, nausea, epilation and erythema fall under the category of symptomatology and are described in Section 2. Lymphocyte depression is a large-scale blood dosimetry marker, and is discussed in Section 3. Of interest to this section are *in-vitro* biological indicators based upon genetic expression and cytogenetics.

Cytogenetics is a relatively active dosimetry field. There are a number of classifications of genetic-level biodosimeters, with the most popular being:

- Chromosome Aberration Analysis (CAA) – counting dicentrics, rings, and possibly fragments.
- Fluorescent In-Site Hybridization (FISH) – can detect CAA aberrations as well as translocations. Advantage is that dicentrics are removed more rapidly that translocations (2 yrs vs. 6 yrs).
- Premature Chromosome Condensation (PCC) – allows determination of dose even when there are no metaphases (high dose), by stimulating (via chemicals) the dying chromosomes to go into metaphase. Can also be used for low-dose to improve statistics.
- Micro-Nucleus Assay (MNA) – essentially counting the small cell nuclei created by fragments (as opposed to complete chromosomes).

The above techniques are all applications of chromosome aberration analysis[2]. The current threshold of dose estimation is approximately 100 cGy.

Actual dose estimates are made by comparing the frequency of specific cytogenetic aberrations in cultured blood lymphocytes of a victim exposed to ionizing radiation with the frequency observed in human lymphocytes irradiated *in vitro*. The central assumption is that if the important *in vivo* exposure conditions can be duplicated *in vitro,* quantitative response of the lymphocytes, at least in chromosome aberration induction, will be identical.

Three kinds of factors influence the accuracy of the *in vitro* dose-response relation determinations and thus the accuracy of the estimated dose for individuals involved in radiation exposure:

- biological aspects of the human lymphocyte system;
- statistical aspects of the data collection; and
- physical conditions of the radiation exposure.

All three factors can affect the viability of any of the biological dosimetry tests for use in physician-assistant software, and are considered below.

4.2.1 Biological Factors

Lymphocytes are relatively uniform in radiosensitivity, relatively long-lived and circulate rapidly throughout the body, which make them prime candidates for biological dosimetry markers (Dufrain, 1980). The cells are synchronized in a post-mitotic, pre-DNA state, which leads to the uniform radiosensitivity and the induction of chromosome type abnormalities. Although a variety of aberrations are induced by radiation, a two-break asymmetrical chromosome type exchange, the dicentric chromosome with accompanying fragment, is now accepted as the standard for human radiation dosimetry. Even more complicated chromosome exchange is possible. In

Figure 16, spectral karyotype staining has been used on radiation damaged blood to identify the dicentrics. The fragments are readily identified, and a combined image is presented in Figure 17. It may be seen that the body of chromosome 6 has fragments from both chromosome 4 and 13 incorporated.

[2] Novel biodosimetry techniques may become the most important area of research in upcoming years for radiation accident investigation. For example, Enzyme Linked Immuno Sorbent Assay (ELISA), which examines gene products (extra-cellular proteins) known as cytokines is being investigated. Since cytokines can show up in bodily fluids (such as saliva) after radiation insult, they become very powerful, non-invasive, field deployable biodosimeters.

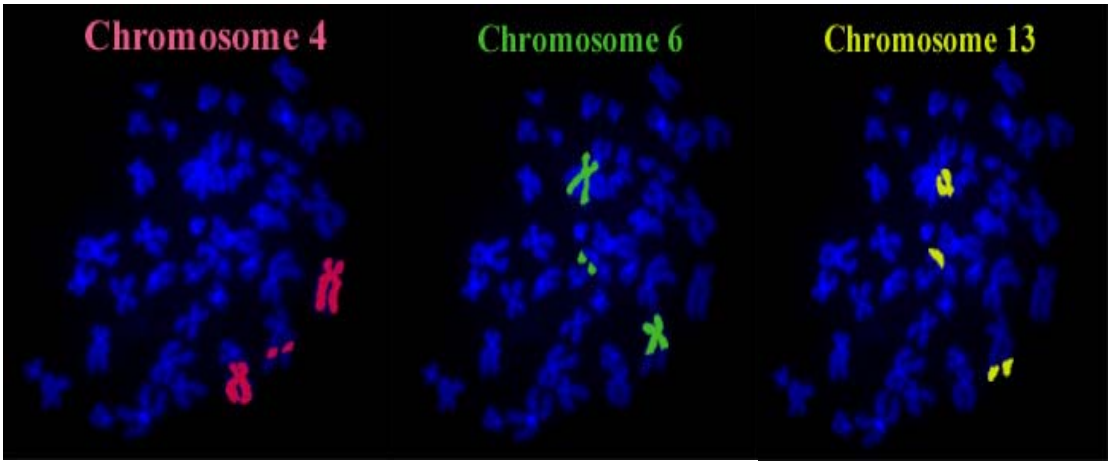

Figure 16 – Spectral karyotyping radiation damaged chromosomes 4, 6 and 13

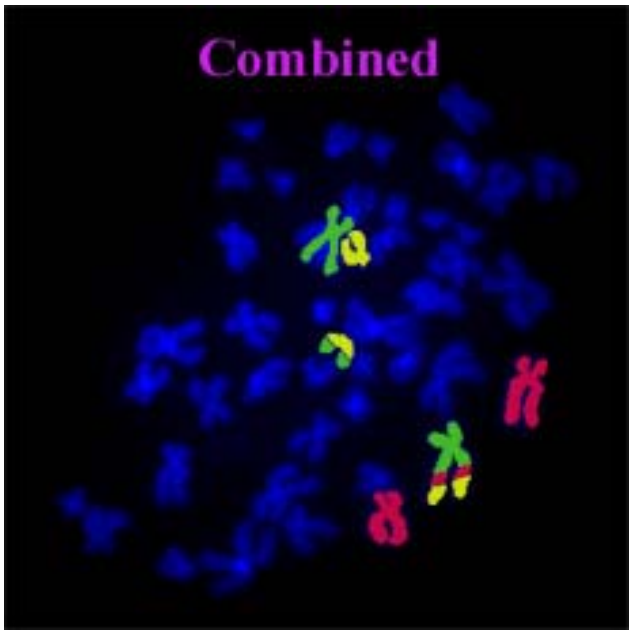

Figure 17 – Chromosome 4, 6 and 13 stains combined into one image

Because human T lymphocytes are long-lived, blood can be drawn for dosimetry up to several weeks after exposure without significant loss of the lesion bearing lymphocytes. The rapid circulation of the lymphocytes through the body tends to integrate the dose and makes possible estimates of whole-body equivalent dose following exposure to penetrating low-LET radiation. These factors are important aspects of the lymphocyte system, and along with the ease of obtaining blood samples and the standardized lymphocyte culture methods are primary reasons that the peripheral lymphocyte has become the most common human biological dosimeter.

4.2.2 Statistical Factors

Several mathematical considerations are important in developing the *in vitro* dose response systems and in applying these results to actual cases of accidental exposure. Initially, the appropriate underlying distributions for the aberration data need to be determined and confirmed. Since chromosome aberrations are random events, their distribution in cells is adequately described by a Poisson distribution, in which the mean is equal to the variance[3]. It has been shown that metaphases from irradiated human lymphocytes follow a Poisson distribution for both low-LET and some forms of high-LET radiation. Partial body exposures to low-LET radiation, non-uniform irradiation from internal deposition of radionuclides and neutron radiation causes over-dispersion of dicentrics. Problems that may be encountered when performing a statistical test for a cytogenetic analysis are different shapes of dose response curves for different qualities of radiation, and possible dependences on dose rate. For example, different dose response curves determined for various radiation types to be used with dicentric chromosome aberration analysis are seen in Figure 18 (DuFrain, 1980).

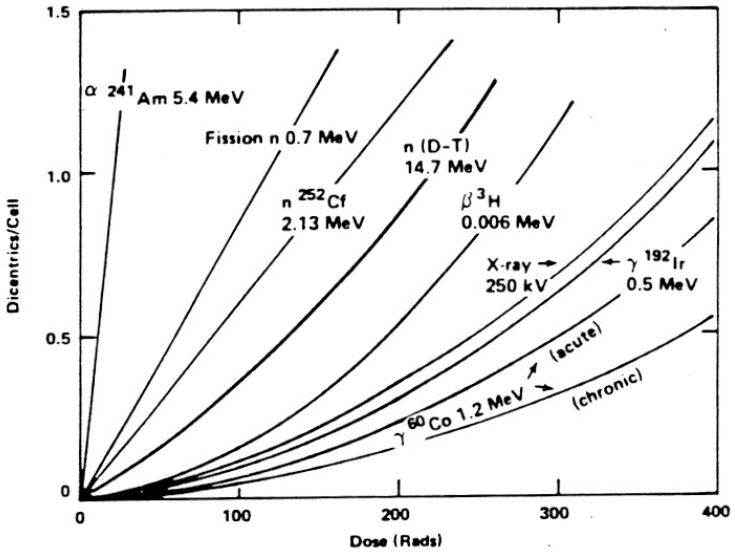

[3] The main ramification of this is that statistics based on the normal distribution where the mean and variance are assumed to be independent are not appropriate for analysis.

Figure 18 - Dose-response curves for dicentric chromosomes

4.2.3 Physical Factors

As discussed in Section 4.2.2, the shape of the dose response curve has an impact on understanding cytogenetic dosimetry. The two primary physical aspects of radiation exposure of human lymphocytes pertain to radiation quality and delivery. Radiation quality can be roughly divided into two components as far as cytogenetic dosimetry is concerned. These are low-LET penetrating radiation, and high-LET radiation which may be penetrating (i.e. neutrons) or of limited range (alpha particles). In general, high-LET radiation results in linear dose-response curves. The linear dose-response model is:

$$Y = \alpha D$$

where Y is the number of dicentrics/cell, α is the slope coefficient of the curve; and D is the absorbed dose. Low energy neutrons follow this linear response, although as neutron energy increases the model requires a second term (quadratic, see equation below). The cytogenetic explanation for the quadratic dose-response curve is that some dicentrics are caused by single energy deposition events, while others are caused by the interaction of two events (thus increasing with the square of the dose). As a rule, as the neutron energy increases the LET falls and the energy deposition becomes less dense along the track of the neutron leading to the quadratic relationship.

Dose-response relations for acute doses of low-LET radiation are described by a quadratic of the form:

$$Y = \alpha D + \beta D^2$$

since the energy deposition events are widely scattered. An example of characteristic curves for both low and high LET radiation is provided in Figure 19. It may be seen that for the same number of measured aberrations per cell, the dose estimate will be different depending upon the LET of the radiation. In this example, the relative biological effectiveness of neutrons over photons is estimated as 2.5 (that is, 2.5 times more gamma dose is required to do the same biological damage as the equivalent neutron dose).

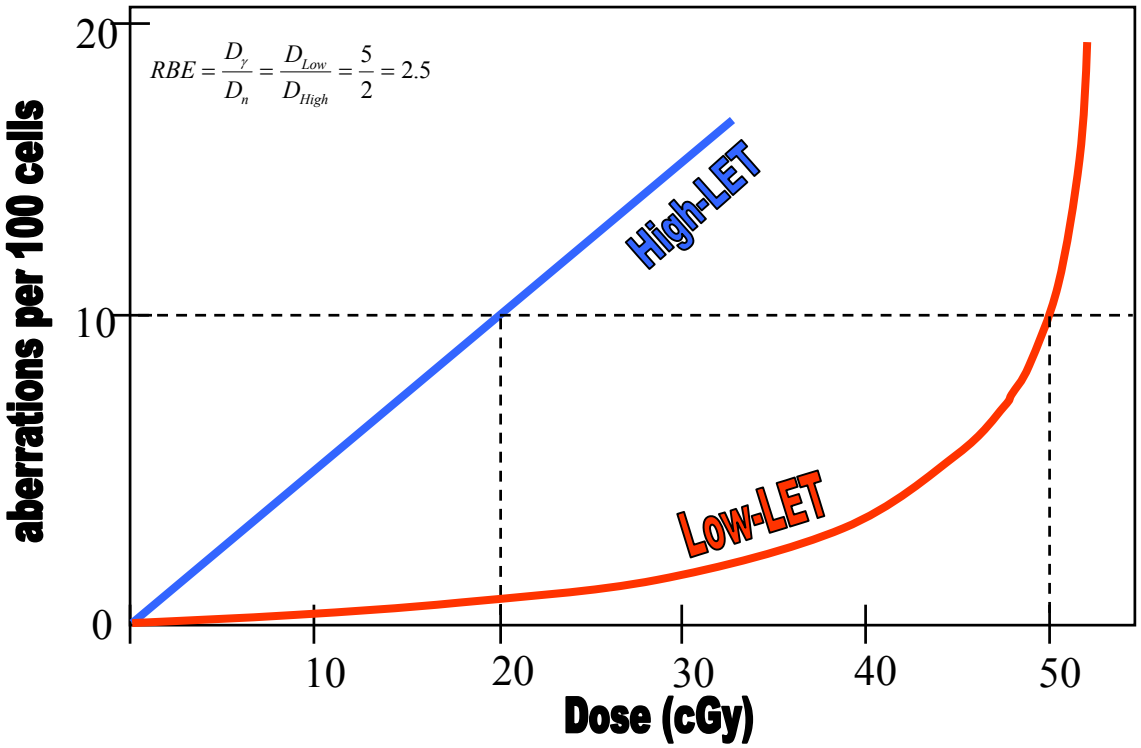

Figure 19 - Chromosome aberrations for low and high LET radiation

4.3 Opportunistic Dosimetry

Opportunistic dosimeters are items that can be used as dosimeters in an emergency. These items are important because they were are passive and present during the accident Several opportunistic dosimeters are available after a criticality accident. It is now considered routine to measure the activation of the victim's body, blood, hair, etc.(see Section 4.1.6). Measurements are also made of items on the person's body or nearby. These include items such as teeth fillings, coins, rings, etc. This information may help to establish the neutron spectrum and the distribution of the radiation exposure.

Following the 1979 Three Mile Island reactor accident, the U.S. Bureau of Radiological Health purchased unexposed film from stores in the surrounding area and analysed the film for exposure. They were able to report that the total exposure at the stores was minimal because the film had received less than 50 μSv (Cloutier, 1990).

Large doses of radiation will darken clear glass. This property of glass was used to evaluate the chronic exposure that occurred in Mexico when a ^{60}Co source of 155 GBq was accidentally located in a home. In addition to darkening, some glasses have the property of emitting visible radiation when stimulated with ultraviolet radiation. After an exposure to ionizing radiation, the amount of visible radiation emitted is related to dose.

Several other methods of obtaining dose information are possible. When radiation interacts with solid matter, it causes minute changes in the electron structure. Most changes are not long-lasting but some are and can be exploited for dosimetric data. Many crystaline materials are capable of providing an adequate thermoluminescent signal long after the exposure. This technique has been used to examine the dose from the atomic bomb by measuring the thermoluminescent signal from roof tiles long after the exposure. The technique has also been used to examine the thermoluminescent properties in items worn by accident victims. Investigators have estimated the dose to radiation accident victims by measuring the thermoluminescent emission from the jewels in each person's watch. This measurement was in good agreement with the reconstructed dose estimate. Unfortunately, the quartz oscillator in modem watches does not have sufficient thermoluminescent properties to be used for radiation accident dosimetry. However, the thermoluminescent properties of dental restoration porcelains can be used for dosimetry.

Another technique involves measuring the number of free radicals produced during a radiation exposure. The radicals (unpaired electrons) can be detected by a technique called electron spin, or paramagnetic, resonance (ESR; EPR). This technique is also discussed in Section 4.1.5. The magnitude of the ESR signal is directly proportional to the magnitude of the radiation exposure. Investigators have measured ESR induced in the nitroglycerin tablets carried by a victim during an accident, and obtained satisfactory dosimetry results. In addition to measuring materials, it has been shown that measuring the ESR signal from both the inside and outside surface of teeth can separate an accidental dose from dental exposures (Aldrich, 1988). ESR has also been used to measure the radiation-produced signal in the cotton cellulose fibers of clothing.

High-LET radiation passing through plastic creates a damage track that can be visualized after etching with a caustic material. The technique is routinely used for monitoring alpha particles and neutrons. The most widely used plastic is called CR-39. Plastics similar to CR-39 are used in digital watches and eyeglasses and after an accident may be a source of additional information on the neutron exposure.

4.4 Dosimetry Comparisons

As discussed in the previous sections, there are a number of methods available after an inadvertent exposure that will allow a dose estimate to be made. For the various methods available, a subjective assessment of the cost, expertise required, time required to perform the test, and lower limit of detection has been made and are presented in Table 8.

Table 8 - Practical comparison of dosimetry techniques[4]

Metric	Cost	Expertise	Time to perform test	Lower limit of detection
Physical dosimetry				
TLD	$10/badge	Technician	15 minutes	100 μSv
EPD	$500/unit	User	Immediate	1 μSv
Survey	Few hundred $	User/Technician	15-30 minutes	few μSv/hr
WB count	Few hundred $	Technician	30 minutes	Variable
Urinalysis	$10-$20/sample	Technician	45 minutes	100 Bq/L
Na-24 (blood)	Few thousand $	Technician/Expert	60 minutes	150 mGy
Biological dosimetry				
ESR	Few thousand $	Expert	24 hours	100 mGy
CAA	Few thousand $	Expert	1 week	100 mGy
PCC	$5k-$10k	Expert	1^+ week	50 mGy
FISH	$5k-$10k	Expert	1^+ week	50 mGy
MNA	~ $10k	Expert	1^+ week	10 mGy
Opportunistic	Variable	Expert	1^+ week	Variable

It may be seen in Table 8 that the most accurate and cost effective method of dosimetry is physical dosimetry, as would be used by Nuclear Energy Workers (NEW). However, radiation dosimetry is often required for people who are not badged, as is often the case under accident conditions. For this case, biological dosimetry is clearly the best choice, as it is a direct indicator of radiation damage.

The higher costs related to biological dosimetry are related to the time required for personnel to process the samples and analyze the results (not included in the estimates are equipment costs – except for EPDs). Therefore, it may be seen that any future improvements in the ability to obtain biological dosimetry estimates *in-situ* will be reflected in lower costs for processing and therefore improved ability to administer the test to large numbers of personnel.

[4] The values presented in the table are subjective and highly dependent upon the laboratory performing the analysis. The values should, therefore, be used only for relative comparative purposes and not for quantitative estimation of cost for a particular test.

5. Bioassay

Bioassay is the determination of the kind, quantity, location and/or retention of radionuclides in the body by direct (*in vivo*) measurement or by indirect measurement of material excreted or removed form the body (*in vitro*). Accurate bioassay measurements are necessary to correctly assess internal exposure to radioactive materials[5].

With respect to the above, bioassay will only be used if an intake of radionuclides is suspected, or if there has been an external neutron exposure.

The following samples may be required to obtain viable bioassay results:

- Urine
- Feces
- Nasal swipes
- Nasal blows
- Sputum
- Sweat
- Breath
- Hair
- Na-24 in blood

In practical terms, considering requirements for a physician-assistant computer code, two examples are provided. For other radionuclides and tests, specific protocols and algorithms must be generated, although the methodology remains the same. A design parameter of the physician-assistant computer code will be whether it is more suitable to enter raw data (such as bioassay result – i.e. "x" Bq/L in a urine sample) or to only allow the committed dose estimate to be entered as a parameter. In theory, it should be possible to allow both methodologies to be used, although this may lead to confusion in the field.

5.1 Bioassay Example 1 – Tritium in urine sample

In this scenario, it is assumed that a person exposed to an inhalation tritium environment has provided a urine sample 14 days after the anticipated exposure, and it is desirable to estimate the committed dose.

Conditions

- Urine assay ~ 6 kBq/litre
- Time after exposure to sample ~ 14 days

[5] Is must be noted that external exposure to neutrons may be detected/quantified by *in-vitro* Na-24 gamma counting of blood.

Assumptions

- Average tritium beta energy ~ 0.006 MeV
- Reference Man contains 42 litres of body fluids
- 47% of the body's daily water intake is via the urinary tract
- Reference man is 70 kg

Calculations

The amount of tritium eliminated in the urine on day t following an accidental exposure is given as follows (Cember, 1992)

$$U(t) = 0.032(A_0)e^{-\lambda_e t}$$

where :

- U(t) is the amount of tritium measured in the urine at time t (Bq)
- t is the time from exposure to sample (days)
- A_0 is the activity at time = 0 (Bq)
- λ_e is the effective elimination constant (~ 0.069 $days^{-1}$ for tritium w/ biological half-life ~ 10 days)

For Reference Man, the initial activity is therefore given as

$$A_0 = \frac{(6\ \text{kBq/litre})(42\ \text{litre})}{0.032} e^{0.069(14)} \approx 20\ \text{MBq}$$

The corresponding inital activity concentration about 490 kBq/litre.

The dose rate, assuming a uniform tritium distribution throughout the body, is given as

$$D_0 = \frac{A_0 \cdot \overline{E} \cdot (1.6 \cdot 10^{-13}\ \text{J/MeV}) \cdot (8.64 \cdot 10^4\ \text{sec/day})}{\text{M} \cdot 1\,(\text{J/kg})/\text{Gy}}$$

where :

- D_0 is the dose rate (Gy/day)
- A_0 is the initial activity (Bq)
- E is the average beta energy (MeV)
- M is the organ mass (kg)

For a tritium uptake, the target organ is the whole body. The dose rate is therefore given as

$$D_0 = \frac{20 \cdot 10^6 \,\text{Bq} \cdot 0.006 \,\text{MeV} \cdot 1.6 \cdot 10^{-13} \,\text{J/MeV} \cdot 8.64 \cdot 10^4 \,\text{sec/day}}{70 \,\text{kg} \cdot 1 \left(\text{J/kg}\right)/\text{Gy}} = 2.37 \cdot 10^{-5} \,\text{Gy/day}$$

Now, the total committed dose is given by

$$D = \frac{D_0}{\lambda_e} = \frac{2.37 \cdot 10^{-5} \,\text{Gy/day}}{0.069 \,\text{day}^{-1}} = 3.43 \cdot 10^{-4} \,\text{Gy} = 0.343 \,\text{mGy}$$

Confirmation

Now, as a confirmatory check, Burnham (1992) quotes the following rule of thumb for tritium uptake

$$Dose = n \left(\text{MBq/litre}\right) \cdot \frac{55 \,\mu\text{Sv/day}}{0.95 \,\text{MBq/litre}} \cdot t \left(\text{days}\right)$$

where :

- n is the average activity concentration from urine analysis (MBq/L)
- t is the time between urine sample analysis (days)

As a conservative estimate, assume that the activity concentration at time = 0 commits a uniform dose for the first day. The dose rate is therefore

$$Dose = 0.49 \,\text{MBq/litre} \cdot \frac{55 \,\mu\text{Sv/day}}{0.95 \,\text{MBq/litre}} = 28.4 \,\mu\text{Sv/day}$$

which gives a committed dose of about 400 μSv (~ 0.4 mGy). This number is consistent with that calculated in the previous section.

The total dose commitment from the tritium uptake is about 340 μGy (0.34 mR). The yearly allowable whole body dose is 1 mSv for a member of the general public. This exposure is therefore about 1/3 of the yearly allowable whole body dose to a non-radiation worker. There should be no observable biological effects from an exposure of this magnitude, and therefore no medical consequences due to this exposure are expected.

5.2 Bioassay Example 2 – Na-24 in blood after neutron irradiation

The body contains several elements that become radioactive when exposed to neutron radiation. The activation of body sodium can be used to make a fairly good estimate of the absorbed dose. Stable ^{23}Na captures thermal neutrons, producing ^{24}Na:

$$^{23}Na(n,\gamma)^{24}Na$$

Sodium-24 has a half-life of 15 hours and emits beta particles (maximum energy ~ 1.4 Mev) and two gamma photons (approximately 2.8 and 1.4 MeV) in cascade. Stable ^{35}Cl and ^{37}Cl are also activated by thermal neutrons[6]. Chlorine-35 produces ^{36}Cl ($t_{1/2}$ ~ 3.0E+05 y), and ^{37}Cl produces ^{38}Cl ($t_{1/2}$ = 37 min) when exposed to neutrons. Chlorine-36 is a pure β emitter, and ^{38}Cl produces β and γ radiation. The neutron dose is proportional to the quantity of ^{24}Na produced in the blood.

The absorbed dose (cSv) from neutrons by counting blood can be calculated using the following relationship:

$$\text{Dose(cSv)} = \frac{A_{\text{Na-24}}\,(\text{Bq})\,\text{per 10 cc whole blood}}{5}$$

where A_{Na-24} is the activity of the sodium-24 in 10 cc whole blood (dps, or Bq). It should be noted that this method of dose estimation is based upon whole body exposure to unmoderated fission neutrons. The neutron dose will vary with both neutron spectrum and body orientation.

Example

Assume a 10 cc blood sample from a victim that has been irradiated by a fission neutron spectrum is counted on a properly calibrated HPGe system, and an activity of 1 kBq ^{24}Na is estimated. The neutron biological dose is estimated using the above relationship as 200 cSv (200 Rem).

[6] Although most neutrons produced in criticality accidents are fast neutrons, they become thermalized through interaction with surrounding materials and the victim's body.

6. Computations

There are numerous approaches for performing dose reconstruction using computational methods. If the source type, activity, position (external), incorporation path (internal), and exposure time can be estimated, then detailed calculations of the dose can be made. There are hundreds of health physics codes available to assist in dosimetric reconstruction. The three major classifications of computation (analytical, deterministic and Monte Carlo) will be briefly discussed along with sections on material cross-sections and dose conversion factors. A section on anthropomorphic phantoms that may be used in accident reconstruction is also included.

6.1 Analytical

Analytical (or semi-analytical) methods for dose reconstruction can either be computational or *rules-of-thumb*. Of prime interest here are the rules-of-thumb, because they have been developed to provide simple to use evaluations of dose in the field. In addition, they have been developed closely with observations, and therefore in many ways can provide the best estimate of dose soon after an accidental exposure. Analytical equations and *rules-of-thumb* are be found in numerous references (see, for example, Schlein, 1998) and are not repeated here. Rules-of-thumb will be an integral part of physician-assistant software.

6.2 Deterministic

The following are brief descriptions of the other major types of calculation methods for neutron and gamma transport. The deterministic techniques are typically only used when calculating neutron or gamma fluence, and then converting it to a biological or absorbed dose using fluence-to-dose conversion factors.

6.2.1 Diffusion Theory

Diffusion theory is used to solve the Boltzmann transport equation by neglecting the detailed directional aspects of particle motion. By expressing the transport simply as particle balancing and making some broad assumptions, the diffusion equation may be derived. The assumptions for diffusion theory are (a) scattering is isotropic in the laboratory frame of reference, (b) particle flux density is nearly isotropic, (c) the medium must be a poor absorber, and (d) results are not valid near boundaries, sources of particles, or sinks. Diffusion theory provides accurate results for infinite, non-hydrogenous media with few energy groups. This method is not readily used for radiation accident dose reconstruction.

6.2.2 Point Kernel Techniques

The point kernel technique uses Green's functions to determine the response of a detector at a space point due to a unit point source of radiation. The kernel for the calculations is usually some combination of attenuation factor, density, build-up factor, energy, flux, and source term. Although there is discussion in the literature about kernel techniques for neutron transport, the point kernel technique has applicability for gamma transport only. A point kernel calculation is most useful for three-dimensional gamma shielding calculations, because it is much faster than other methods for similar accuracy. The most common commercial software available for performing point kernel gamma transport is Microshield, which has been used for radiation accident dose reconstruction.

6.2.3 Discrete Ordinates

Discrete ordinates is a solution to the Boltzmann transport equation using discretized variables. The steady-state Boltzmann transport equation for the directional flux density $\psi(r,\mu,E)$ may be written in standard notation as

$$\Omega \cdot \nabla \psi(r,\Omega,E) + \sigma_t(r,E)\psi(r,\Omega,E)$$
$$= \int_0^\infty dE' \int_{-1}^{1} d\Omega' \left[\chi(E)\upsilon\sigma_f(r,E') + \sigma_s(r,\Omega' \longrightarrow \Omega, E' \longrightarrow E)\right]\psi(r,\Omega',E') + Q(r,\Omega,E)$$

where the macroscopic cross sections have been denoted with a lower case σ to prevent confusion between macroscopic cross sections and the summation symbol Σ. It has been assumed that there is one fission spectrum $\chi(E)$ for all materials.

If the above equation is multiplied by drdΩdE, the transport equation becomes a statement of particle balance for the phase-space differential element drdΩdE. The first term on the left represents the net streaming of particles out of the differential element. The second term on the left represents the loss of particles from the element by collision (eg. absorption and scatter). The first term on the right represents the gain of particles into the differential phase-space element by either fission or scattering events. Finally, the last term on the right represents particles gained into the element from the external fixed sources.

Numerical solution of the transport equation by the discrete ordinates method requires discretization of the energy dependence (E) and (E') of the fission spectrum, cross sections, fluxes, and source. It also requires discretization of the angular variable Ω and the angular dependence (Ω) of the scattering cross section, fluxes, and source. Finally, the spatial operator (∇) and the spatial

dependence (r) of the fluxes, cross sections, and source must also be discretized.

The energy dependence is discretized in a multi energy group approximation. The angular variable, Ω, and the angular dependence (Ω) of the fluxes and source are discretized in the discrete ordinates approximation. However, the angular dependence ($\Omega' \rightarrow \Omega$) of the scattering cross sections is represented by an orthogonal Legendre polynomial expansion. The spatial operator (∇) and the spatial dependence (r) are discretized in the finite difference approximation.

6.3 Monte Carlo

Monte Carlo analysis is often thought of as a computer "experiment". The method employs random numbers to select probabilities of particle interactions along with resultant energies and directions of particle flight after collisions. Monte Carlo codes are usually written for three-dimensional geometries and are capable of supporting complex geometrical definitions. Using this type of code, all elements of geometry can be fully described in three dimensions, and the simulation is effectively acting similar to an experiment. The critical information required to set up a Monte Carlo model is, in general, listed as:

- All dimensions;
- All materials (elemental composition and bulk density);
- Source specifications; and
- Detector specifications (position and type).

When a source particle is created, it has properties of position (x,y,z), direction (u,v,w) and energy (E). Most source particles (electrons) will interact with the target, and the subsequent photons produced (again with some x,y,z,u,v,w,E) will generate neutrons through photoneutron interactions. The photoneutrons become a secondary source (or, for this study, the source of interest) and each neutron is born with its own (x,y,z,u,v,w,E). The probability of a particle collision with a material depends upon the abundance of a given material (or element), and the cross-section (or interaction probability) at a given energy. In Monte Carlo, pseudo-random number generators are used to determine how each particle interacts, and what the fate of the particle will be.

The main advantages to using Monte Carlo analysis over discrete ordinates are that if used properly, Monte Carlo can give very accurate results, and calculations can be improved upon simply by continuing a previous calculation. The main disadvantages are that Monte Carlo analysis is time consuming (although this is less of an issue with fast computers available today), and the codes are usually designed for an experienced user (due to the simulation of complex three-dimensional geometries). There are a number of computer codes available that have been used for radiation accident

reconstruction. Some of the more useful Monte Carlo codes used are described as follows.

6.3.1 MCNP

The Monte Carlo Neutron Photon (MCNP) code was developed by Los Alamos National Laboratory (LANL) and performs **neutron, photon and electron** Monte Carlo transport for particle energies less than about 20 MeV (typically). MCNP uses an arbitrary geometry representation by constructing complicated structures using surfaces and Boolean operators. The latest MCNP version is 4C.

6.3.2 MCNPX

This code, based upon MCNP, allows the user to perform particle transport from GeV energies down to a minimum cut-off energy, without having to run numerous codes to obtain the results. The code is capable of transporting the following particles: **nucleons, pions and muons**. The code contains several features not available in MCNP, including integration of the LAHET Code System (LCS) for high energy (>20 MeV) interactions. The most recent complete beta version of MCNPX is 2.4.j, and this code is arguably the state-of-the-art in high-energy nucleon transport codes.

6.3.3 SABRINA

This code is used for visualization and verification of 3-dimensional geometries in which MCNP and other codes (such as LCS and MCNPX) simulate the transport of radiation. Ray tracing is the primary method for generating images. Sabrina can perform geometry error checking, display the tracks of Monte Carlo simulated particles, and translate solid body geometry to MCNP surface geometry. This tool is invaluable both for verification of complex geometry and presentation of results.

6.3.4 EGS

The Electron Gamma Shower (EGS) code performs **electron and photon** transport using Monte Carlo methods. It utilizes generalized geometry routines, including the Combinatorial Geometry (CG) package. It is more powerful than the ITS system described below, but is also much more complicated to use.

6.3.5 ITS

The Integrated TIGER Series (ITS) is a series of codes to transport **electrons and photons** through simple geometries using the Monte Carlo method. The constituent codes are TIGER for one dimensional, CYLTRAN for two

dimensional, and ACCEPT for three dimensional transport. When the above codes end in "P", they have improved ionization and relaxation atomic shell models. When the above codes end in "M", they take into account the effects of magnetic fields (CYLTRAN and ACCEPT only).

6.4 Cross-Section Libraries

The accuracy of a transport calculation is highly dependent on the selection of a cross section set. Cross section data has historically been derived by a combination of experimental measurements and theoretical calculations. Raw nuclear data can exist in various forms depending upon the experiments and calculations carried out (ref: Nuclear Reactor Analysis). It was therefore decided many years ago to consolidate the available nuclear data so that it may easily be updated and allow broad availability to nuclear analysts. As a result, the Evaluated Nuclear Data File (ENDF) was established.

The Evaluated Nuclear Data File (ENDF) system was developed for the storage and retrieval of evaluated nuclear data for applications in nuclear technology. The formats and libraries are coordinated by the National Nuclear Data Center (NNDC) and decided upon by the Cross Section Evaluation Working Group (CSEWG), which is a collaborative effort by national laboratories, industry, and universities in the U.S., as well as Chalk River Laboratory (CRL) in Canada. It is also well to note that there are other evaluated cross section sets used by various national laboratories and countries, however these all are related back to the ENDF system. There are three computer libraries associated with the ENDF system.

1. CSISRS (Cross Section Information Storage and Retrieval System) This data set contains unevaluated raw data from experimental measurements. This data is essentially of no use for running transport codes.

2. **ENDF/A -** This data set contains both complete and incomplete sets of nuclear data as soon as they become available. For certain isotopes there may be more than one set of nuclear data, pertaining to different experimenters or different experiments. Although this data is the most recent, it has not been fully tested, and therefore may be in error. Unless the most recent data is absolutely required, this data should not be used for transport calculations.

3. **ENDF/B -** This data set contains complete and evaluated cross section set, with only one recommended evaluation for each isotope. The ENDF/B format is the standard for nuclear reactor calculations in North America. There is a great deal of effort required to prepare cross section data in the ENDF/B format. Collecting, organizing, checking for consistency, filling gaps, and presenting the data is an enormous task. The actual data contained in the ENDF/B file is not in tabular form, but rather in the form of

numerous fitting parameters that can be assembled by a processing code. The latest version of the ENDF/B library is ENDF/B-6.

To obtain cross section sets for use in a transport calculation, the ENDF/B data must be manipulated by a processing code into a fully evaluated set of cross sections as a function of energy. The processing code is able to interpret the parametrized data contained in ENDF/B, and reconstruct cross sections to the needs of the user. For example, if Doppler broadened cross sections are needed, the processing code can generate these from the ENDF/B parameters.

6.5 Dose Conversion Factors

There are a number of dose conversion factors available for neutron and photon interactions in tissue. The most recent and well-documented evaluations may be found in ICRP-74 (ICRP, 1996), which are derived from ICRP-60 recommendations (ICRP, 1991). For electrons, the average energy deposition in a region of tissue (by energy balance) can be calculated directly, and an estimate of absorbed dose made directly. This methodology, which can be applied to all particle interaction types, is best used in cases when charged particle equilibrium does not hold. The condition of charged particle equilibrium may not be fulfilled (a) in the vicinity of an interface between two different materials – especially near an air-material interface, (b) near the edges of a beam or in regions very close to a radiation source, (c) when there is a large change in photon spectrum with depth of penetration, and (d) when a high-energy photon beam is incident on high-Z material.

6.6 Phantoms

Two primary phantom model methodologies are available for representing a human body tissue in Monte Carlo calculations. These are voxelized phantoms, which are based on CT or MR images of actual humans and tissues, and mathematical models where body contours and organs are defined by mathematical expressions.

6.6.1 MIRD Mathematical Models

Most of the computational models of the human body commonly in use are the so-called mathematical models: mathematical expressions representing planes, cylindrical, conical, elliptical or spherical surfaces are used to describe idealized arrangements of body organs. This type of model was introduced by Oak Ridge National Laboratory for the adult human (Eckerman, 1996). Several pediatric models were derived to represent infants and children of various ages and male and female adult mathematical models were developed. For all of these models, the organ volumes are in

accordance with the ICRP data on Reference Man (ICRP, 1975). The paradigm of the mathematical models is commonly called the "MIRD-5 phantom", due to being published in the MIRD Pamphlet No. 5. Referring to this, mathematical models are often called MIRD-type models.

6.6.2 Voxelized Geometrical Phantoms

Recently, tomographic models have been developed, which use computed tomographic (CT) or magnetic resonance (MR) data of real persons to provide three-dimensional representations of the body. The first step for the construction of these models is to obtain CT or MR scans consisting of contiguous slices of tissue, or even the whole body. The data are then processed using appropriate image processing software. Each organ or tissue is represented by those volume elements (voxels) which were identified as belonging to it from the CT or MR slice images. This tomographic type of model is called a voxel (volume pixel) model. Recent work has been performed by SAIC Canada for DREO in developing voxelized hand models for use in MCNP, based upon MR images (SAIC 2002).

6.6.3 Comparison of Mathematical and Voxelized Phantom Models

In mathematical models, organ shapes are reduced to a very simple form to limit the software and computational requirements. Consequently, the mathematical models are not designed to describe any individual in detail but rather to represent whole populations. On the other hand, tomographic models are constructed from CT or MR data of real persons who might deviate significantly from reference data. The shapes of the body organs are determined by identifying all the voxels belonging to each organ. Thus, the shape of each organ is more realistic than for the mathematical models, although, being reconstructed from a specific individual, it might not be representative of large populations. Mathematical models are usually rigid in size, whereas the external dimensions of tomographic models can be adapted to any size, for each of the three dimensions independently. All internal dimensions of the resulting scaled-down or scaled-up version of the original model are also changed with the same scaling factors. It is, however, important to keep the scaling factors within rational magnitudes; otherwise, considerable errors in the body proportions might be introduced. In mathematical models, all skeletal components are homogeneously distributed in the skeleton. Although it is not possible to identify functional bone marrow by this method or to model the complicated trabecular bone structure exactly, the distribution of bone marrow can be determined with the resolution of CT or MR scans (normally a few mm^3). Apart from these differences, considering the overall aims and limitations, the two types of models, mathematical and tomographic, are, in principle, equally suitable for the calculation of organ and tissue doses. Radiation transport in the human phantoms is usually calculated using Monte Carlo codes following individual

particle histories. For each single particle history, the parameters influencing its actual course are selected randomly from their probability distributions. There are libraries of cross section data for the radiation interaction processes (see Section 6.4) for all elements from which the cross section data for body tissues are then evaluated according to their elemental composition and density. Organ absorbed doses are evaluated by summing, in each organ and tissue, all energy depositions from primary and secondary particles and dividing by the organ mass. This results in the average absorbed dose in the organ regardless of the irradiated fraction.

7. Data Interpretation for Radiation Dose Reconstruction

7.1 Methodology

The ability to make an accurate medical prediction of accidental radiation dose exposure must be examined in two realms: human factors and technical. For example, the ability to obtain meaningful radiation injury information from data fusion relies upon (a) understanding of both the technical issues related to the operation of a given piece of dosimetry equipment along with the signals obtained, and (b) human factors issues with respect to operator understanding and interpretation of the data presented. The overall goal is to reduce the number of false positives for a given medical threat assessment, while simultaneously ensuring that the no radiation exposures go undetected.

A presentation of methods and models for radiation dose decision in complex systems is given in Figure 20. It may be seen that qualitative methods are based more on human factors analysis, whereas quantitative methods are based more upon probabilistic algorithms. The broad field of information science is an attempt to merge the two aforementioned areas. Many of the concepts presented will be investigated for the fusion of the dosimetry information.

7.2 Categorization

7.2.1 Orthogonality

The concept of orthogonality address how "different" various information parameters are from one another, in terms of what information they provide and how they provide it. For instance, two individual physical dosimetry estimates compared to each other would not be as orthogonal as a physical dosimetry estimate compared with a computational dose estimate. Similar systems are, by design, not highly orthogonal, and are prone to similar systematic errors, whereas non-similar systems can provide independent threat assessment. The former case provides redundancy for a single technology type, thereby improving the reliability of a single technology, whereas the latter case provides an improved probability of threat detection. It is therefore advantageous, in general, to have orthogonal systems.

Examples of orthogonal and non-orthogonal systems are given in Figure 21. As may be seen, a non-orthogonal system has overlap in the type of data, and therefore has overlap in the parameter being measured. An orthogonal system, on the other hand, does not overlap on type of data, although it may be found to overlap in the parameter being measured.

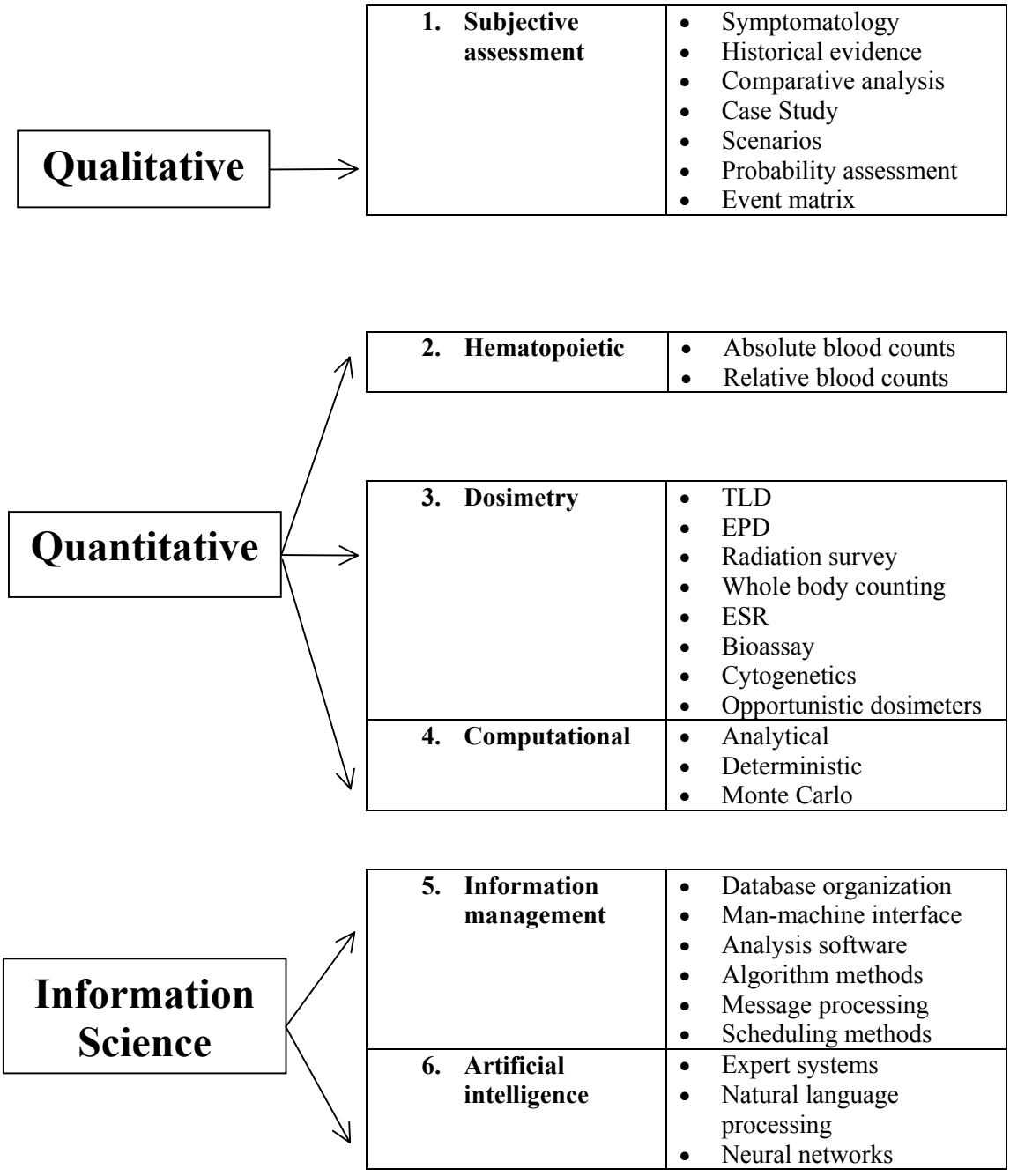

Figure 20 - Methods and models for decision analysis

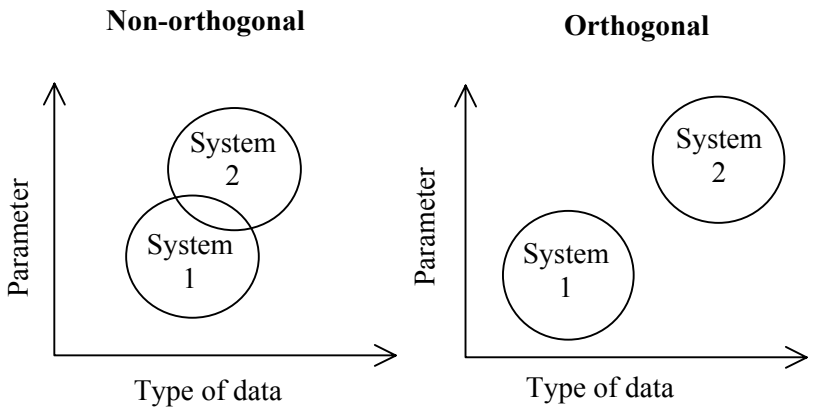

Figure 21 - Descriptive of orthogonality in phase space

All information metrics identified must be categorized with respect to orthogonality. This enables the identification of the independent (primary) parameter for assessment and the supporting (secondary) parameter(s) for improved decision making.

7.2.2 Automation

The degree of automation for computer aided dosimetry for dose reconstruction relates to the amount of human operator interaction required for making a medical assessment. For example, currently practiced dose reconstruction has relatively low levels of automation, since an operator is vital to the dose assessment.

Each system identified may have numerous decision parameters, each with varying levels of automation. For this project, system parameters that have high levels of automation and simultaneously high confidence levels are very important to real-time data fusion. In some cases, improvements in the levels of automation may be achieved by subtle changes in the way the data from interacting systems is collected and utilized.

7.2.3 Data Fusion Methodologies

An example of the general pattern for multi-input data integration and fusion in a system may be seen in Figure 22. It may be seen that there are an arbitrary number of sensors integrated to provide information to the system, and while the fusion of information takes place at the nodes, the entire network structure together with the integration functions are part of the multi-input data integration process. By way of an example of how the fusion works, the following scenario is presented:

- The outputs x_1 and x_2 from the first two sensors are fused to form a new representation $x_{1,2}$. For example, the "symptoms" and "physical dosimetry" fuse the medical indications and available experimental dose estimate.
- The output from a third sensor x_3 could then be fused with $x_{1,2}$, to obtain the relationship $x_{1,2,3}$. For example, "computation" fuses simulation data with the previous level.
- The output $x_{1,2,3}$ may then be fused at nodes higher in the structure.
- In addition, the output from all sensors may be integrated into an overall representation

The data fusion can be performed using simple logic rules, or more complex modeling, such as neural networks.

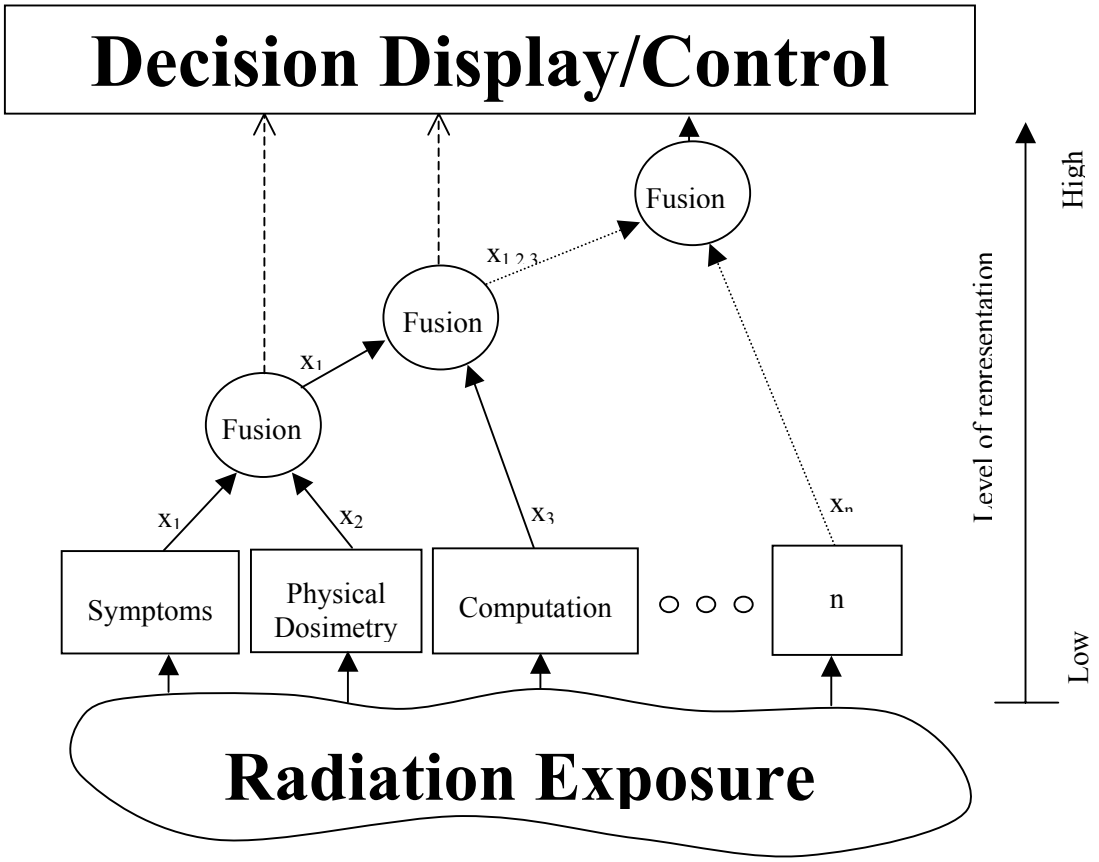

Figure 22 - Data fusion example

7.2.4 Decision Assignment

The act of deciding whether a given set of conditions represents a radiation dose can be very complicated. The process of fusing numerous data inputs for providing an enhanced assessment of a dose must consider both the data available and the operator's ability to judge the data. In all cases, decision rules must be applied to determine the level of dose threat.

Of vital importance to the data fusion is the type of data provided. Overall, radiation dose reconstruction involves both soft and hard data. Some examples are:

Soft data	**Hard data**
Symptomatology	Physical dosimetry
History	Bioassay
Simulation	Hematology
Other	*Other*

As seen above soft data may be considered data that may provide an indication of radiation exposure but is not conclusive on its own. Hard data, on the other hand, may be considered data that provides relatively conclusive proof that an exposure has occurred.

7.3 Verification of Accuracy

An important aspect to the CADAVER physician-assistant model is the verification of dose accuracy. Accuracy refers to the quality of the information provided by the classification scheme, and is distinguished from the usefulness of the information. To evaluate the accuracy of the CADAVER models, it is possible to use three different approaches that have been used in clinical decision-making:

- Decision Matrix;
- Receiver Operator Characteristic Curve; and
- Information Theory.

The three approaches (described below) may be of value for verifying CADAVER efficacy.

7.3.1 Decision Matrix

A decision matrix is typically applied to simple decision, i.e. whether a person has been exposed or not (McNeil, 1975). A simple decision matrix for radiation exposure is formed from the following questions:

- Are the indicators (symptoms, dicentrics, etc) present (I+) or absent (I-)
- Has there been radiation exposure (E+) or no exposure (E-)

And is expressed in matrix form as (Lusted, 1971):

Indicator	**Exposure**	
	E+	**E-**
I+	a	c
I-	b	d

The four (4) matrix combinations can be used to evaluate a test for the presence or absence of radiation exposure.

The true-positive ratio (TP), expressed the ratio of persons tested that have actually been exposed, and have some abnormal (or characteristic) indicator. The expression of this conditional probability P is given as

$$TP = P(I+|E+) = \frac{a}{a+b}$$

The true positive ratio is an expression of the **sensitivity** of the indicator, and measure the fraction of persons exposed that are detector by the indicator. The false positive (FP) is given as

$$FP = P(I+|E-) = \frac{c}{c+d}$$

and is the probability that persons not exposed will have indicators that suggest exposure.

The true negative (TN) ratio is the proportion of negative indicators in all persons that have not been exposed, and is expressed as

$$TN = P(I-|E-) = \frac{d}{c+d}$$

The true negative ratio is an expression of the **specificity** of the indicator, and measures the fraction of persons who will be correctly identified as not having been exposed. This indictor is also (*1-FP*). The false negative test (FN), which expresses the number of persons who have been exposed but have negative indicators, is given by

$$FN = P\left(I - \middle| E + \right) = \frac{b}{a+b}$$

and is equal to (*1-TP*).

A good diagnostic indicator for radiation injury should have a high TP ratio and a small FP ratio. The ratio of TP to FP is sometimes called the likelihood ratio (L), and indicators with high likelihood ratios are better indicators than those with low ratios.

7.3.2 Receiver-Operator Characteristic (ROC) Curves

Although the decision matrix method can be applied individually to each indictor (i.e. nausea, lymphocyte depletion, etc), it is not suitable to determine the overall behavior of the data fusion indicators (i.e. all indictors). Assuming that they have differing sensitivities and specificities to identify radiation insult, a receiver-operator characteristic (ROC) curve can be generated. Numerous studies have been published on the usefulness of ROC curves (see, for example, Lusted (1971), McNeil (1975), Zweig (1993) and DeLeo (1993)).

A general characteristic of the ROC curve is that as the true positive ratio (sensitivity) increases, so does the false positive ratio (1-specificity), as depicted in Figure 23. The importance of this is that it allows determination of a cutoff point for analysis, and depicts how additional (or more sensitive) indictors affect the data fusion. For example, it is clear in Figure 23 that to the right of the dashed line, there are increasing false positives for additional increase in true positives. A decision must be made as to whether the false positive cost (in terms of time and money) is worthy of the increase in true positives. In the CADAVER model, it is proposed to consider the dose assessment elements as points on an ROC curve.

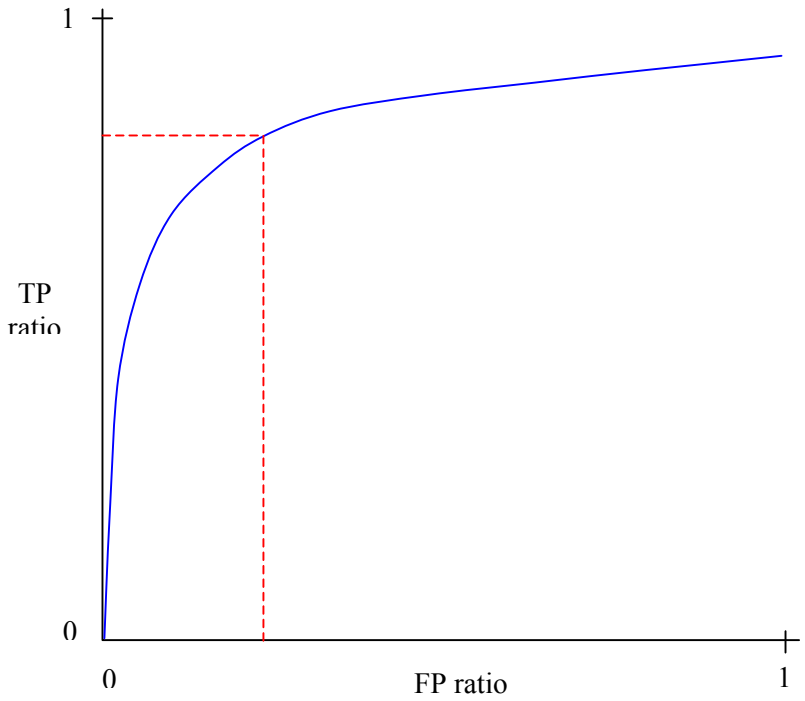

Figure 23 - Ideal ROC curve

7.3.3 Information Theory

Information theory has been used as a possible means of selecting a cut-off point along the ROC curve (McNeil, 1975). In this context, information may be defined as a reduction in uncertainty, and the greater the difference between uncertainty of the estimated exposure after a test is performed and the certainty before it was performed, the greater the information in the test. There are numerous types of information theory applications that may be applied to the CADAVER model verification. One of the most powerful methods is detection limit statistics.

Decisions analysis is governed by the statistics of detection (or, detection limit statistics). The purpose of detection limit statistics is to provide a quantitative estimate of the probability that, given a net signal over some background, there is positively net signal present (Chambless, 1992). The main application of detection limit statistics is when the signal is small with respect to the background.

There are two statistical limits considered and applied to signal detection; the critical limit L_c and the detection limit L_d. In general, the errors being minimized when performing small signal analysis are: false positive error (type I) - claiming that there is a signal present when in fact there is not, and false negative error (type II) - claiming that there is no signal present when in fact there is a signal. It is clear to see that a type I error is on the side of conservancy, while a type II error is on the side of catastrophe.

The probabilities for type I and type II errors are based on Gaussian statistics (Currie, 1968). The Gaussian (or Normal) function is given as follows:

$$P = \frac{1}{\sqrt{2\pi}} \int_k^\infty e^{-x^2/2} dx$$

The probability is obtained by integrating the Gaussian with a limit of integration denoted k. Figure 24 depicts the probability functions for both detection and false alarm probabilities, and are applied to the statistical limits.

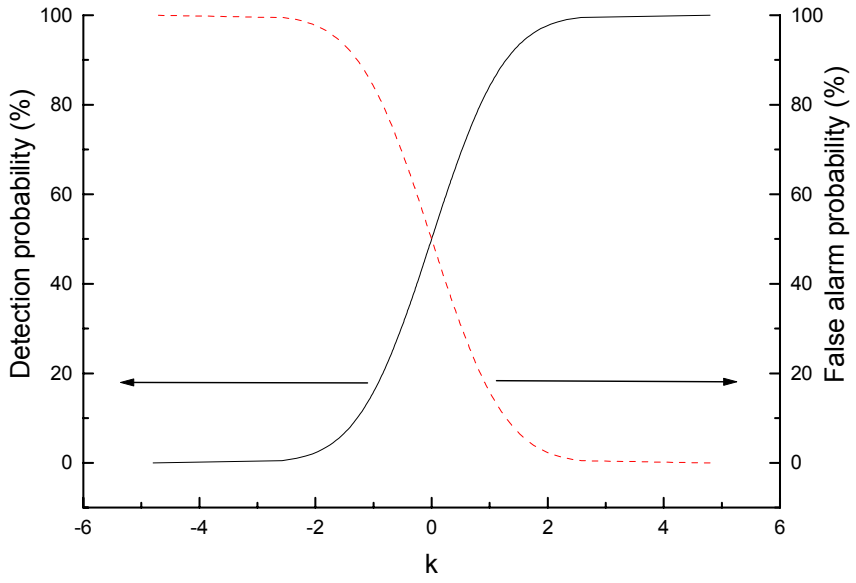

Figure 24 - Gaussian probability functions

The first statistical limit is called the critical level (L_c) and is the critical value below which it may be assumed that the net signal is due to statistical background fluctuations and above which we may say a signal has been detected due to true net signal. The equation for the critical limit, assuming no net activity and a single measurement, is given as:

$$L_c = k_\alpha \left(2\sigma_b^2\right)^{1/2}$$

where L_c is the critical level, k_α is the variate of the probability distribution for false alarm, and σ_b^2 is the background signal.

It may be seen that for a given confidence level and background, a unique critical limit exists such that a net count above the calculated level is considered to be due to net signal with probability α. The false alarm probability (probability that the net signal measured is due to background fluctuations) may therefore be quoted as $1-\alpha$.

The second statistical limit is called the detection limit (L_d) and is the level above which it may be certain that the net signal is larger than the critical level, with a confidence $1-\beta$. In this way $1-\beta$ is defined as the detection probability. Net signal measured above L_d are certain to be detected and reported as a positive result. By this definition, L_d may be considered the minimum detectable signal. The above suggests a relationship between L_c and Ld, given as:

$$L_d = L_c + \frac{k_\beta^2}{2}\left\{1+\left(1+\frac{4L_c}{k_\beta^2}+\frac{4L_c^2}{k_\alpha^2 k_\beta^2}\right)^{1/2}\right\}$$

where L_d is the detection limit (counts), and k_β is the variate of the probability distribution for detection.

It may be seen that the detection limit is a fixed level above the critical level, and an inherent function of the critical level.

There are two important cases to consider for the application at hand, namely 1) allowing an *a prioi* acceptable false alarm probability (setting k_α), and 2) allowing the false alarm probability to be equal to the complement of the detection probability ($k_\alpha = k_\beta = k$). Statistically, the background is a Gaussian distribution in signal around 0, and the true signal is a Gaussian distribution around the detection limit. This concept is best illustrated in Figure 25. As may be seen, the probabilities α and β lie on either side of L_c, and the measured net signal is therefore distributed between the false alarm and detection probabilities.

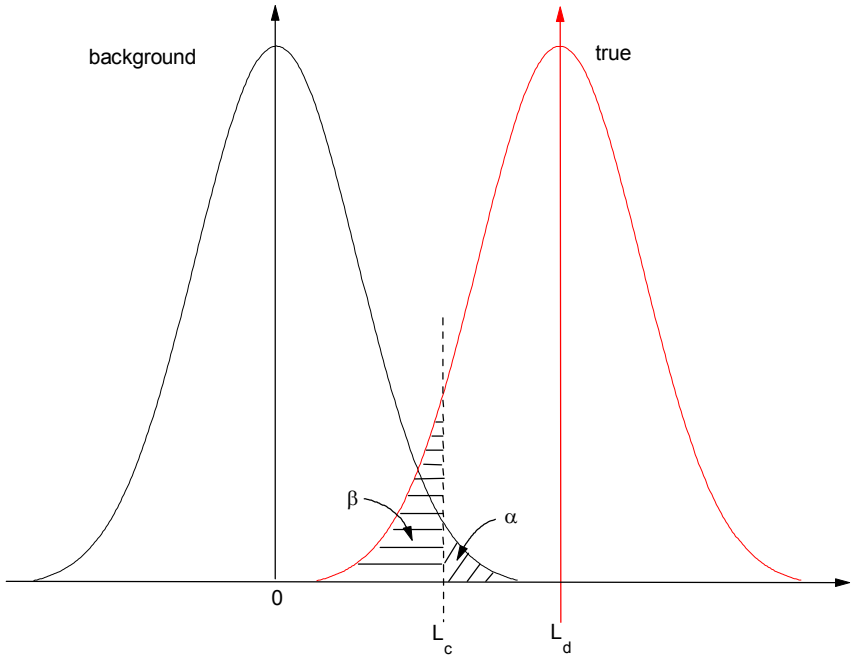

Figure 25 - Overlapping Gaussians depicting the distribution of net signal

In case 1 above, an explicit expression for k_β cannot be determined, as it is a function of probability. Therefore, L_d is calculated with a fixed k_α and L_c based upon the required false alarm probability, while L_d is calculated as a function of k_β (hence the detection probability). The net counts are compared to L_d until they are equal, and therefore the detection probability for a fixed false alarm probability is found.

In case 2 above, an explicit expression for L_d can be derived for $k_\alpha = k_\beta = k$. An expression for L_d is given as

$$L_d = 2L_c + k^2 = 2k\left(2\sigma_b^2\right)^{1/2} + k^2$$

which, when re-arranged for k gives

$$k = -\sqrt{2\,\sigma_b^2} + \sqrt{2\,\sigma_b^2 + L_d}$$

It may be readily seen that if the detection limit is set equal to the net signal, the value of k (and therefore detection probability) is found immediately. In this case, the false alarm probability is simply the complement of the detection probability.

The difference in the two approaches is that in case 1 the user is allowed to define an acceptable false alarm probability to determine the detection probability, while in case 2 the false alarm probability is determined *a posteriori*. The advantage of one approach to the other is dictated by the users need to keep the Gaussians separate or not. For large excess signal, a single Gaussian as is used in case 2 is suitable. For scenarios when the excess signal is approaching zero, the case 1 method may be more appropriate.

Bayes theorem is a well-used concept in probability theory (McCormick, 1981). If P(A) is used to represent the probability of an event A, and P(B) is used to represent the probability of an event B, the probability of event A occurring given that event B has occurred may be given as:

$$P(A \mid B) = P(A)\left[\frac{P(B \mid A)}{P(B)}\right]$$

where P(B | A) is the probability that event B has happened given event A happened.

Now, if A' is defined as an event A that has not occurred (that is to say, a false positive) and P(A') as the probability that we determine A has occurred when in fact it has not, we can define the probability of the occurrence of event B using Bayes theorem as :

$$P(B) = P(B \mid A)P(A) + P(B \mid A')P(A')$$

because either A or A' must happen, but not both.

Re-arranging the above equations gives:

$$P(A \mid B) = \frac{P(A)}{\left[P(A) + \frac{P(B \mid A')P(A')}{P(B \mid A)}\right]}$$

Now, using the fact that P(A') = 1 - P(A) and substituting variables a modified Bayes equation (generally termed Matthew's formula) is obtained:

$$P(A \mid B) = \frac{p}{[p + r(1-p)]}$$

where p = P(A) and r = P(B | A') / P (B | A).

The variable **r** represents the ratio of false to true determination. That is to say, the numerator is the probability that a signal will be detected with a given probability when in fact there is no signal (termed false alarm probability) whereas the denominator is the probability that a signal has been detected to a given probability given that there is a signal present.

It may be seen that Bayes theorem may be utilized to determine the probability that when a person has an abnormal test result, they actually have been exposed (McNeil, 1975).

8. Strawman for CADAVER Data Fusion

The Strawman for the CADAVER physician-assistant model is provided in Figure 26.

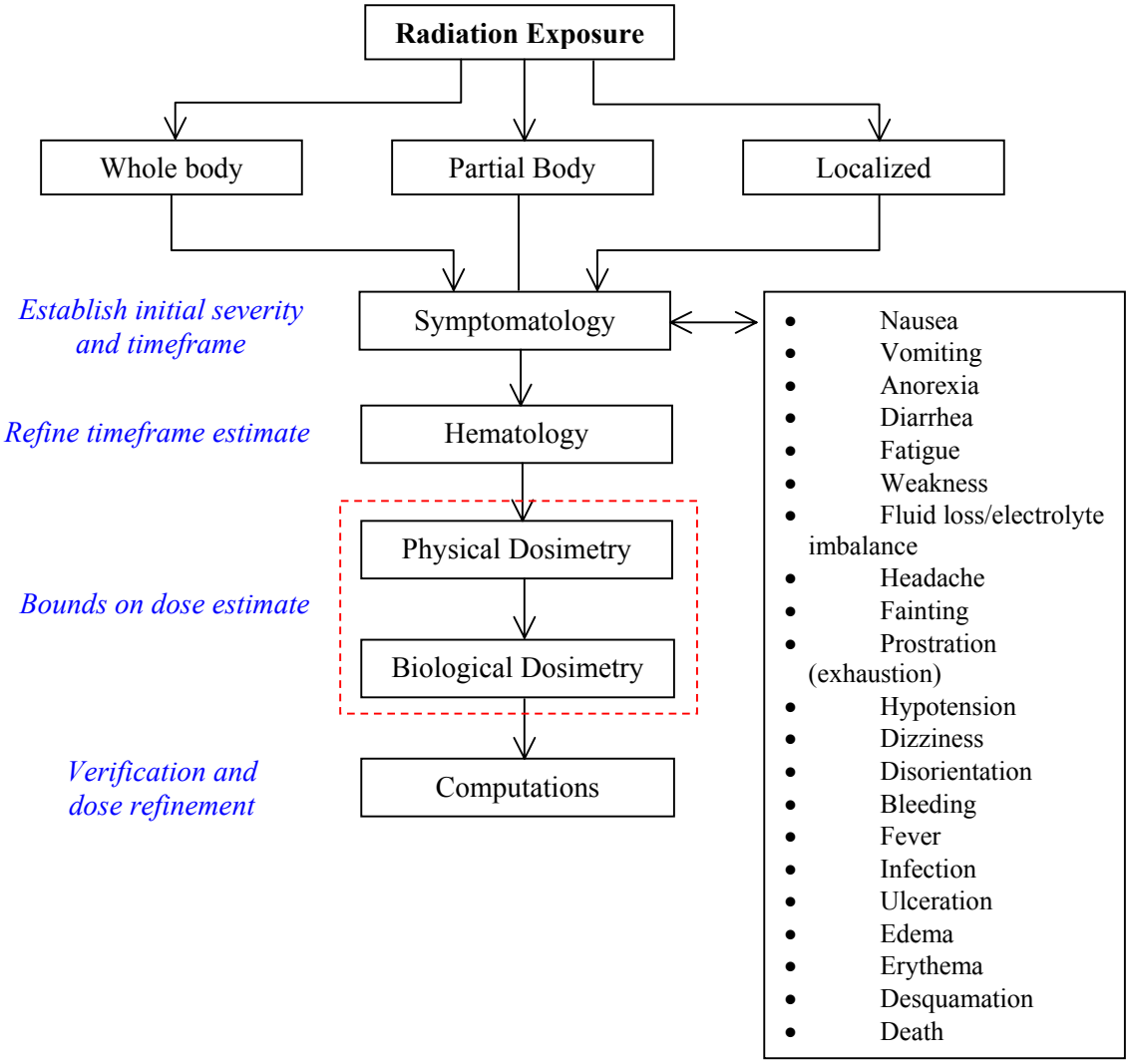

Figure 26 - Strawman diagram for CADAVER model

It may be seen that moving down the Strawman suggests increasing time. For example, it is assumed that symptoms will be observed before a computational model is generated[7].

In terms of orthogonality of fusion components, the five (5) major decision elements: symptomatology, hematology, physical dosimetry, biological dosimetry and computational dose reconstruction are all orthogonal, since the dose estimates obtained from each are all independent. Within each element, some sub-elements are orthogonal and some are not. For example, nausea and vomiting would not be considered orthogonal because they are sequential forms of the same end-point (nausea precedes vomiting usually).

In the following tables, all non-orthogonal members are grouped together, and each orthogonal element is in it's own column. For symptomatology, Table 9 shows that there are six (6) different orthogonal classifications.

Initially, for blood components, all three primary indicators could be considered orthogonal, since they have differing response trends to the same insult. However, it is observed that the thrombocytes and neutrophils exhibit similar trends on the order of 2 weeks after a severe insult, and therefore can be considered to be non-orthogonal. In addition, the neutrophils and lymphocytes are both members of the leukocyte family, and therefore are not completely independent. Therefore, Table 10 presents the blood data as being a single element, with three non-orthogonal sub-elements.

For the dosimetry (both physical and biological), the orthogonal groupings are presented in Table 11. The table has been grouped in terms of passive dosimetry techniques, and intrusive techniques (where some portion of the potentially exposed personnel or surroundings must be analyzed, usually in a laboratory). It may be seen that nasal swipes, blows and sputum are orthogonal to the other intrusive methods for obtaining an internal dose estimate, mainly because they are only indicators of an intake, and not uptake (which causes the dose). Also, novel cytogenetic methods may in fact be orthogonal to the other cytogenetic methods, depending upon how the test is performed. The orthogonality of cytogenetics with other blood work (for example, lymphocyte depletion) is assumed, but may not always hold true. For example, persons undergoing radiation therapy treatment will have both depressed lymphocytes and chromosome aberrations. In an acute radiation accident however, the lymphocyte depletion kinetics will change, as will the chromosome aberration population. It is likely that in this scenario, the data will still be orthogonal because of the extreme lymphocyte change.

[7] Although this is generally true, there may be instances when this assumption does not hold. For example, a computational estimate may be available before bioassay results.

The orthogonality for computational methods of dose reconstruction is shown in Table 12. The Monte Carlo method is grouped as being orthogonal to the analytical and deterministic only when voxelized, or MIRD-based, phantoms are used in the modeling. This is due to the fact that when realistic phantoms are used in conjunction with Monte Carlo, the results are similar as if a laboratory experiment has been conducted, whereas the other methods provide global dose estimates, suitable as first approximations.

The orthogonal sets may be used in a data fusion algorithm to provide an increasing improved estimate of the dose after accidental exposure.

Table 9 - Orthogonality groupings for symptomatology

Fluid	Energy	CNS	WBC	Skin	System
Nausea Vomiting Anorexia Fluid loss/electrolyte imbalance Diarrhea	Fatigue Weakness Fainting Prostration (exhaustion)	Headache Hypotension Dizziness Disorientation	Fever Infection	Ulceration Edema Erythema Desquamation	Death

Table 10 - Orthogonality groupings for hematopoietic indicators

Blood component	Comment
Thrombocytes	*These become non-orthogonal with time*
Neutrophils	***Leukocyte family***
Lymphocytes	

Table 11 - Orthogonality groupings for dosimetry

Passive External	Passive Internal	Intrusive External	Intrusive Internal		Cytogenetics
TLD EPD Survey Whole Body Opportunistic	Whole Body	ESR Na-24 blood	Urine Feces Sweat Breathe Hair Na-24 blood	Nasal swipes Nasal blows Sputum	CAA PCC FISH MNA Novel methods

Table 12 - Orthogonality groupings for computational methods

Non-Specific	Specific
Analytical Deterministic	Monte Carlo

9. Conclusions and Recommendations

9.1 Conclusions

After a radiation accidental exposure, there are a number of short, medium and long-term indicators of the severity of the exposure. For both civilian and military operations, it is of prime importance to make early assessment of the biological dose to personnel, since this has implications to triage, fulfillment of military objectives, allocation of resources, etc. Data that indicates severity of exposure comes typically from five primary groupings: symptomatology, hematology, physical dosimetry, biological dosimetry, and computational dose reconstruction. Since the groupings are generally from varied areas of expertise (medicine, radiobiology, health physics, etc), it is desirable to have a protocol to utilize the diverse information to allow reasonable military and medical decisions to be made.

This report has outlined some of the general aspects of the data required for use in physician-assistant software (termed the CADAVER model). It is expected that a computational tool would be utilized from the initial radiological event until the patient has initiated full recovery, or succumbed to injuries. Other groups have performed research in this field for military applications (Sine, 2001), however this framework is the first to include computational dose reconstruction, an increasing powerful tool for dose severity estimation. In addition, the proposed CADAVER model is designed upon a data fusion framework, as opposed to only collecting, presenting and archiving data. In this way, the software to be developed would be in the form of an intelligent system.

Within the context of this report, some areas pertinent, but ancillary, to radiation injury have not been addressed, such as privacy of medical information (within the context of the model) and confounding injury (such as thermal or blunt trauma). Although these issues are important, they do not directly affect the assessment of radiation insult severity. Although they have not been discussed herein, they are important nonetheless and would be considered as part of a computer code package. For example, the symptomatology for radiation injury would be linked to data obtained about non-radiation injury, which would affect the usefulness of the data (as an example, consider the inhalation of a radioactive cloud which also contains a chemical weapon agent; some symptoms will be caused by both insults).

The feasibility of the CADAVER model is made possible by relatively recent advances in computational power. It is certain that such software can be developed and implemented on a laptop personal computer, which makes field portable radiation accident severity diagnosis a reality for military operations in hostile environments.

9.2 Recommendation

Based upon the work herein, the following ten (10) recommendations are presented:

1) Software with GUI should be developed based upon the five (5) primary dose severity indicators, that uses statistical and data fusion principles, to allow real-time assessment of biological dose and severity of exposure.

2) Simplification of blood dynamics differential equations should be investigated for inclusion into the software.

3) Neural network data analysis (back-propagation) should be considered as part of the data analysis algorithm (at least as an analysis option).

4) Assessment as to whether raw data (to enable calculation of a committed dose), computer data (i.e. calculated committed dose) or both be used as input parameters to the software.

5) Bayesian probability estimators should be investigated for incorporation into the CADAVER model. If the CADAVER model (or elements of the model) is used with some success under different scenarios, the *a posteriori* probabilities may be calculated for each test. This in turn can become a metric within the CADAVER model.

6) Methodology for inclusion of Monte Carlo modeling should be considered for the software (i.e. direct integration or job spawning).

7) Synergy of radiation and non-radiation insult should be investigated, and incorporated into the software.

8) The interface software should be developed in a GUI-friendly format (such as Visual Basic), and computationally intensive models be programmed in FORTRAN or C/C++.

9) The five (5) primary dose severity indicator handling should be coded as self-contained modules to the greatest possible extent, for ease of modifying, debugging and testing. The data fusion algorithm(s) should be independent modules as well.

10) Data should be compiled to satisfy as many of the metrics outlined in Table 9 through Table 12, for as many radiation accidents as possible. Some data should be set aside for testing the CADAVER model, while the majority of the data should be utilized for programming elements of the data fusion models (such as neural network training and Bayesian estimation).

10. References

1. AFRRI (1996) Triage of Irradiated Personnel, Armed Forces Radiobiology Research Institute Workshop Proceedings, AFRRI Special Publication 98-2, 25-27 September.

2. Aldrich (1988) "Determining Radiation Exposure from Nuclear Accidents and Atomic Tests using Dental Enamel", Aldrich, J.E. and Pass, B., Health Phys., Vol. 54, No. 4.

3. Andrews (1973) "Hematologic Data for Estimating Injury in Radiation Accidents", Andrews, G.A., International Workshop on Recent Advances in Medical Management in Radiation Accidents, Washington.

4. Andrews (1980) "Medical Management of Accidental Total-body Irradiation", Andrews, G.A., in The Medical Basis for Radiation Accident Preparedness, Hubner, K.F. and Fry, S.A., Editors, Elsevier North Holland Inc.

5. Anno (1989) "Symptomatology of Acute Radiation Effects in Humans after Exposure to Dose of 0.5 – 30 Gy", Annon, G.H., Baum, S.J., Withers, H.R. and Young, R.W., Health Phys, Vol. 56< no.6.

6. Burnham (1992) Radiation Protection, by Burnham, J., New Brunswick Electric Power Corporation.

7. Cember (1991) Introduction to Health Physics – Second Edition, by Cember, H., McGraw-Hill, Toronto.

8. Chambless (1992) "Detection Limit Concepts : Foundations, Myths, and Utilization", Chambless, D.A., Dubose, S.S., and Sensintaffer, E.L., Health Phys., Vol. 63, No. 3.

9. Cloutier (1990) "Radiation Accident Dose Reconstruction", Cloutier, R.J. and Simpson, D.R., in The Medical Basis for Radiation Accident Preparedness II – Cinical Experience and Follow-up Since 1979, Ricks, R.C. and Fry, S.A., Editors, Elsevier.

10. Currie (1968) "Limits for Qualitative Detection and Quantitative Determination", Currie, L.A., Anal. Chem., Vol. 40, No. 3.

11. DeLeo (1993) "Receiver Operating Characteristic Laboratory (ROCLAB): Software for Developing Decision Strategies that Account for Uncertainty", DeLeo, J.M., in Second International Symposium on Uncertainty Modeling and Analysis, IEEE Computer Society.

12. DuFrain (1980) "In Vitro Human Cytogenetic Dose-Response Systems", Dufrain, R.J., Littlefield, L.G., Joiner, E.E. and Frome, E.L., in The Medical Basis for Radiation Accident Preparedness, Hubner, K.F. and Fry, S.A., Editors, Elsevier North Holland Inc.

13. Eckerman (1996) "The ORNL Mathematical Phantom", Eckerman, K.F., Cristy, M. and Ryman, J.C., available at http://homer.ornl.gov/vlab/VLabPhan.html

14. Goans (1997) "Early Dose Assessment Following Severe Radiation Accidents", Goans, R.E., Holloway, E.C., Berger, M.E., and Ricks, R.C., Health Phys, Vo. 72, No. 4.

15. Hofer (1994) "A Clinical Decision Support System for the Treatment of Irradiated Persons Based on a Mathematical Model of Granulocytopoiesis", Hofer, E.P. and Tibken, B., 12th Triennial World Congress of IFAC (Automatic Control).

16. Hofer (1995) "An Approach to a Biomathematical Model of Lymphocytopoiesis", Hofer, E.P., Brucher, S., Mehr, K. and Tibken, B., Stem Cells, Vol. 13(Suppl. 1).

17. IAEA (1988) Medical Handling of Accidentally Exposed Individuals: Recommendations, International Atomic Energy Agency, Safety Series Report No. 88, Vienna.

18. IAEA (1998) Diagnosis and Treatment of Radiation Injuries, International Atomic Energy Agency, Safety Series Report No. 2, Vienna.

19. ICRP (1991) "1990 Recommendations of the International Commission on Radiological Protection", ICRP No. 60,. Annals of the ICRP Vol. 21, No. 1-3.

20. ICRP (1975) "Reference Man: Anatomical, Physiological and Metabolic Characteristics", International Commission on Radiological Protection, ICRP Publication 23, Pergamon Press, Oxford, UK.

21. ICRP (1996) "Conversion Coefficients for use in Radiological Protection against External Radiation", ICRP No. 74, Annals of the ICRP, Vol. 26, No. 3-4.

22. Lusted (1971a) "Decision-Making Studies in Patient Management", Lusted, L.B., New England J. Med., Vol. 284, No. 8.

23. Lusted (1971b) "Signal Detectability and Medical Decision-Making", Lusted, L.B., Science, Vol. 171.

24. McCann (2000) "On the Utility of Experimental Cross-Training for Team Decision-Making Under Time Stress", McCann, C., Baranski, J.V., Thompson, M.M. and Pigeau, R.A., Ergonomics, Vol. 43, No. 8.

25. McCormick (1981) Reliability and Risk Analysis, by McCormick, N.J., Academic Press, New York.

26. McNeil (1975) "Primer on Certain Elements of Medical Decision Making", McNeil, B.J., Keeler, E., and Adelstein, S.J., New England J. Med., Vol. 293, No. 5.

27. NCRP (2001) "Management of Terrorist Events Involving Radioactive Material", National Council on Radiation Protection and Measurements, NCRP Report No. 138, Bethesda, Maryland.

28. Nishikawa (2001) "Computer-aided Diagnosis for Screening Mammography", Nishikawa, R., Canadian Med. Phys. Newsletter, Vol. 47, No. 3.

29. Norman (1991) "Cognitive Science in the Cockpit", CSERIAC Gateway-2.

30. O'Dell (1987) "Transport Calculations for Nuclear Analysis: Theory and Guidelines for Effective Use of Transport Codes", O'Dell, R.D. and Alcouffe, R.E., Los Alamos National Laboratory, LA-10983-MS.

31. SAIC (2002) "Voxelized Models of the Human Hand for Radiation Accident Dose Reconstruction using the MCNP Radiation Transport Code", Waller, E.J., SAIC Canada Task B398-000.

32. Sine (2001) "Biodosimetry Assessment Tool: A Postexposure Software Program for Military Applications", Sine, R.C., Levine, I.H., Glass, J.L., Jackson, W.E., Young, R.W. and Blakely, W.F., Abstract - Armed Forces Radiobiology Research Institute, MD.

33. Tibken (1995) "A Biomathematical Model of Granulocytopoiesis for Estimation of Stem Cells", Hofer, E.P., Brucher, S., Mehr, K. and Tibken, B., Stem Cells, Vol. 13(Suppl. 1).

34. Zweig (1993) "Receiver-Operating Characteristics (ROC) Plots: A Fundamental Evaluation Tool in Clinical Medicine", Clin. Chem., Vol. 39, No. 4.

11. Selected Glossary of Terms

A

Anosmia - loss of the sense of smell

B

b.i.d. - twice per day (*bis in die*)
BAL - British Anti-Lewistite

C

Canthus - corner of the eye in proximity to the ear duct
Catharsis - cleansing or purging
CBC - complete blood count. ***CBC with differential*** means that the blood count has been broken down into components, such as thrombocytes, neutrophils, lymphocytes and hemoglobin.
Ciliary action – motion of fluid in and around the eye caused by the cilia
CNS - central nervous system
Cocci - pertaining to a spherical bacterial cell
Conjunctivitis - inflammation around the eyes, including thick sticky morning discharge
Cornified – thickened skin caused by a buildup of dead epithelium cells
Creatine – a nitrogenous compound formed by metabolic processes in the body
Creatinine – substance formed from the metabolism of creatine, commonly found in blood, urine and tissue

D

d - day
Debridement - to remove dirt, foreign objects, damaged tissue etc from a wound

Decorporation – a chemical acceleration of the removal of radioactive atoms from the body, using chelating agents or other administered pharmaceutical agents (*Health Phys., Vol. 78, No .5, pp. 563-565, 2000*).
Diaphoresis - sweating (*dia+pherein*)
Distal - farthest point away from the centre point or centre-line

Edema - swelling (*oidema*)
Endotracheal - within or through the trachea (*endon+tracheia*)
Epithelium - covering of the internal and external organs of the body (*epi+thele*)
Erythema - reddness (*erythros*)
Eschar - scab or dry crust resulting from a chemical burn, infection, of skin disease
Eutrophication - water rich in plant nutrients but deficient in oxygen

Glomerulus - structure composed of blood vessels or nerve fibres
Gram-positive - referring to a positive indication, via violet stain, of some strands of pathogenic bacteria (Gram-negative refers to bacteria that do not stain violet)
Granulocytopenia – an abnormal condition of the blood, characterized by a decrease in the total number of granulocytes. Also termed neutropenia. (*granulum+kytos+penia*)
Granulocytopoiesis – see Granulocytopenia.
Granulocytosis – an abnormal condition of the blood, characterized by an increase in the total number of granulocytes. (*granulum+kytos+osis*)

Hct - hematocrit
Hgb - hemoglobin
h – hour
Hypotension – an abnormal condition in which the blood pressure is not adequate for normal perfusion and oxygenation of the tissues (*hypo+tendere*)

Hypertonic – having a greater concentration of solute than another solution (for example, a hypertonic saline solution may contain 1 – 15% sodium chloride, as compared to normal saline at 0.9%)

I

i.m. - intramuscular
i.v. - intravenous
inj. – injection
Immunosuppression – an abnormal condition of the immune system characterized by markedly inhibited ability to respond to antigen stimuli (*immunis+supprimere*)
Intake - the quantity of radioactive material entering the body via inhalation, ingestion, absorption or wounds
Intralumenal – inside a cavity or channel within the body

J

K

KI - potassium iodide

L

Lacrimation - excessive amount of tear production
Lavage – washing
Leukopenia – abnormal decrease in the number of white blood cells (< 5000 cells/ mm^3)
Ligand - molecule, ion, or group bound to the central atom of a chemical compound; organic molecule attached to a specific site on a surface.
Lymphopenia – a smaller than normal number of lymphocytes in the peripheral circulation. Also termed lymphocytopenia (*lympha+kytos+penes*)
Lymphocytopenia – see lymphopenia
Lymphocytopoiesis – see lymphopenia

M

N

Nadir - the lowest point
n.p.o. - nothing by mouth (*nihil per os*)
Nebulizer – a device for producing a fine spray
Necrosis - local tissue death (*nekros*+*osis*)
Nephrotoxic – toxic or destructive to the kidney

O

Obstipation - extreme or persistent constipation
Oliguria - diminished capacity to pass urine (*oligos*+*ouron*)

P

Pancytopenia – an abnormal condition characterized by a marked reduction in the number of all the cellular elements of the blood, the red blood cells, white blood cells, and platelets (*pan*+*kytos*+*penia*)
(Intra)peritoneal – into the peritoneal (abdominal) cavity
p.o. - orally (*per os*)
p.r.n. - when required (*pro re nata*)
Prodromal – an early sign of a developing condition; the earliest phase
Pruritus - itching (*prurire*)

Q

q. - each, every (*quaque*)
q.d. - every day (*quaque die*)

R

Renal - pertaining to the kidney
RBC - red blood cell

S

Sepsis - infection (*sepein*)
Stat. - Immediately (*statim*)
Syncope - brief lapse in consciousness (*synkoptein*)

T

t.i.d. - 3 times/day (*ter in die*)
tabl – tablet
Teratogenesis – development of physical defects in the embryo
Thrombocytopenia – abnormally low number of platelets in the blood
Transferrin - trace protein present in blood, essential in the transport of iron. Main function is to move iron from the intestine to the bloodstream.

U

Uptake - quantity of radioactive material transferred from the site of intake to body organs or tissue (uptake is a fraction, up to 1, of the intake)

V

Vasodilation - widening of blood vessels (*vas*+*dilatare*)

W

WBC - white blood cell
Wilson's Disease - rare, inherited disorder of copper metabolism, in which copper slowly accumulates in the liver and is released and taken up by other parts of the body. This disease can affect the brain, liver and kidneys.
Wound - any physical injury causing a break in the skin

X, Y & Z

DOCUMENT CONTROL DATA

(Security classification of title, body of abstract and indexing annotation must be entered when the overall document is classified)

1. ORIGINATOR (the name and address of the organization preparing the document. Organizations for whom the document was prepared, e.g. Establishment sponsoring a contractor's report, or tasking agency, are entered in section 8.)

   Defence R&D Canada - Ottawa
   Ottawa ON KlA 0Z4

2. SECURITY CLASSIFICATION (overall security classification of the document, including special warning terms if applicable)

   UNCLASSIFIED

3. TITLE (the complete document title as indicated on the title page. Its classification should be indicated by the appropriate abbreviation (S,C or U) in parentheses after the title.)

   Computer aided dosimetry and verification of exposure to radiation (U)

4. AUTHORS (Last name, first name, middle initial)

   Waller, Edward; Stodilka, Robert Z; Leach, Karen E.; Prud'homme-Lalonde, Louise

5. DATE OF PUBLICATION (month and year of publication of document)	6a. NO. OF PAGES (total containing information. Include Annexes, Appendices, etc.)	6b. NO. OF REFS (total cited in document)
June 2002	84	34

7. DESCRIPTIVE NOTES (the category of the document, e.g. technical report, technical note or memorandum. If appropriate, enter the type of report, e.g. interim, progress, summary, annual or final. Give the inclusive dates when a specific reporting period is covered.)

   Technical report

8. SPONSORING ACTIVITY (the name of the department project office or laboratory sponsoring the research and development. Include the address.)

   Defence R&D Canada - Ottawa

9a. PROJECT OR GRANT NO. (if appropriate, the applicable research and development project or grant number under which the document was written. Please specify whether project or grant)	9b. CONTRACT NO. (if appropriate, the applicable number under which the document was written)
Project 6qe12	

10a. ORIGINATOR'S DOCUMENT NUMBER (the official document number by which the document is identified by the originating activity. This number must be unique to this document.)	10b. OTHER DOCUMENT NOS. (Any other numbers which may be assigned this document either by the originator or by the sponsor)
DRDC Ottawa TR 2002-055	

11. DOCUMENT AVAILABILITY (any limitations on further dissemination of the document, other than those imposed by security classification)

    (X) Unlimited distribution
    ( ) Distribution limited to defence departments and defence contractors; further distribution only as approved
    ( ) Distribution limited to defence departments and Canadian defence contractors; further distribution only as approved
    ( ) Distribution limited to government departments and agencies; further distribution only as approved
    ( ) Distribution limited to defence departments; further distribution only as approved
    ( ) Other (please specify):

12. DOCUMENT ANNOUNCEMENT (any limitation to the bibliographic announcement of this document. This will normally correspond to the Document Availability (11). However, where further distribution (beyond the audience specified in 11) is possible, a wider announcement audience may be selected.)

    Same as above

13. ABSTRACT (a brief and factual summary of the document. It may also appear elsewhere in the body of the document itself. It is highly desirable that the abstract of classified documents be unclassified. Each paragraph of the abstract shall begin with an indication of the security classification of the information in the paragraph (unless the document itself is unclassified) represented as (S), (C), or (U). It is not necessary to include here abstracts in both official languages unless the text is bilingual).

In the timeframe following the September 11th attacks on the United States, increased emphasis has been placed on Chemical, Biological, Radiological and Nuclear (CBRN) preparedness. Of prime importance is rapid field assessment of potential radiation exposure to Canadian Forces field personnel.
This work set up a framework for generating an "expert" computer system for aiding and assisting field personnel in determining the extent of radiation insult to military personnel. Data was gathered by review of the available literature, discussions with medical and health physics personnel having hands-on experience dealing with radiation accident victims, and from experience of the principal investigator. Flow charts and generic data fusion algorithms were developed. Relationships between known exposure parameters, patient interview and history, clinical symptoms, clinical work-ups, physical dosimetry, biological dosimetry, and dose reconstruction as critical data indicators were investigated.
The data obtained was examined in terms of information theory. A main goal was to determine how best to generate an adaptive model (i.e. when more data becomes available, how is the prediction improved). Consideration was given to determination of predictive algorithms for health outcome. In addition, the concept of coding an expert medical treatment advisor system was developed (U)

14. KEYWORDS, DESCRIPTORS or IDENTIFIERS (technically meaningful terms or short phrases that characterize a document and could be helpful in cataloguing the document. They should be selected so that no security classification is required. Identifiers such as equipment model designation, trade name, military project code name, geographic location may also be included. If possible keywords should be selected from a published thesaurus. e.g. Thesaurus of Engineering and Scientific Terms (TEST) and that thesaurus-identified. If it is not possible to select indexing terms which are Unclassified, the classification of each should be indicated as with the title.)

Radiation
Nuclear
Dosimetry

Defence R&D Canada

Canada's leader in defence
and national security R&D

R & D pour la défense Canada

Chef de file au Canada en R & D
pour la défense et la sécurité nationale

www.drdc-rddc.gc.ca